2016

Effects of digestate, magnesium sulfate, and dipotassium hydrogen phosphate/potassium dihydrogen phosphate on microalga, Scenedesmus dimorphus

Zhuohui Joe He
Cleveland State University

EFFECTS OF DIGESTATE, MAGNESIUM SULFATE, AND DIPOTASSIUM HYDROGEN PHOSPHATE/POTASSIUM DIHYDROGEN PHOSPHATE ON MICROALGA, *Scenedesmus dimorphus*

ZHUOHUI JOE HE

Bachelor of Science in Biochemistry

North Carolina State University

December 2010

Submitted in partial fulfillment of requirements for the degree

MASTER OF SCIENCE IN CHEMICAL ENGINEERING

at

CLEVELAND STATE UNIVERSITY

October, 2016

We hereby approve this thesis

For

Zhuohui Joe He

Candidate for the

MASTER OF SCIENCE DEGREE IN CHEMICAL ENGINEERING

from the Department of

Chemical and Biomedical Engineering

and

CLEVELAND STATE UNIVERSITY'S

College of Graduate Studies by

_____Date_____
Dr. Joanne M. Belovich
Department of Chemical and Biomedical Engineering

_____Date_____
Dr. Jorge E. Gatica
Department of Chemical and Biomedical Engineering

_____Date_____
Dr. Moo-Yeal Lee
Department of Chemical and Biomedical Engineering

October 27th, 2016
Student's Date of Defense

DEDICATION

This thesis is dedicated to NASA Glenn Research Center.

EFFECTS OF DIGESTATE, MAGNESIUM SULFATE, AND DIPOTASSIUM HYDROGEN PHOSPHATE/POTASSIUM DIHYDROGEN PHOSPHATE ON MICROALGA, *Scenedesmus dimorphus*

ZHUOHUI JOE HE

ABSTRACT

Digestate (*D*), the remaining substance after anaerobic digestion of a biodegradable feedstock, is rich in inorganic contents, which makes it a good candidate for growing algae for biofuel production. Previous studies showed digestate at around 1.25% to 1.75% (v/v) dilution is suitable for algae growth. In this study, magnesium sulfate ($MgSO_4$) and dipotassium hydrogen phosphate/potassium dihydrogen phosphate (*K-P*) were added to diluted digestate growth media. Two sets of experiments were conducted in batch reactor mode to identify the digestate (*D*), magnesium sulfate ($MgSO_4$) and dipotassium hydrogen phosphate/potassium dihydrogen phosphate (*K-P*) concentrations that would optimize the algae growth. Algae growth parameters, such as maximum growth rate (r) and maximum algae concentration (X_{max}) were estimated by using non-linear regression with a four-parameter logistic equation. Average biomass productivity (P_a), instantaneous biomass productivity (P_i), and specific growth rate (u_g) were also calculated. This study used a central composite design. A surface response regression equation was generated for each of these algae growth parameters; the equation contained linear terms, quadratic terms, and the first order interaction terms of the three factors (*D*, $MgSO_4$, and *K-P*). The resulting regression models showed both the maximum growth rate and the maximum algae concentrations were mainly dependent on digestate. The highest maximum growth rate was obtained at around 1% (v/v) digestate dilution. Within the tested digestate dilutions (0.184 to 1.817% (v/v)), maximum algae concentration increases with digestate concentration. In addition, the data and analysis showed that

digestate concentration of 1.4% (v/v) dilution and low *K-P* and $MgSO_4$ concentrations would be expected to result in high average biomass productivity and instantaneous biomass productivity. The digestate concentrations does not alter the effects of *K-P* and $MgSO_4$ on algae growth, but an interaction was seen between *K-P* and $MgSO_4$. At low concentrations of these two factors ($MgSO_4$ < 0.61 mmol/L and *K-P* < 2.81 mmol/L), both experiments 1 and 2 showed that lower the *K-P* and $MgSO_4$ concentrations would yield higher maximum growth rate. The cause might be that the additional *K-P* and $MgSO_4$ might promote larger cell production rather than cell replication, or the replicated cells may stay attached, which would lead to slower perceived growth rate but higher maximum algae concentration at the end of the batch growth.

TABLE OF CONTENTS

LIST OF TABLES

LIST OF FIGURES

CHAPTER I

INTRODUCTION

Liquid fuels are stable and have higher energy density than gas fuels, such as hydrogen and methane and are cleaner to burn than solid fuels, like coal. Human daily living today heavily depends on liquid fuels. In 2014, the global liquid fuel consumption was about 92.4 million barrel per day and this number keeps increasing every year (U.S. EIA, 2015). The most economical way to produce liquid fuels today is from fossil fuels underground, or another name, petroleum. Transportation, for example, heavily depends on petroleum liquid fuels, such as gasoline for cars, diesel for trucks, and jet fuel for commercial aircraft. About 95% of transportation fuel comes from petroleum products (Rodrigue & Comtois, 2013). Fischer-Tropsch synthesis is another way to make liquid fuel from solid fuel or gas fuel. This involves a process to convert hydrogen and carbon monoxide gas into higher energy density liquid fuels (Hu et al., 2012). Many energy companies, such as Shell, Rentech, and Sasol, produce liquid fuel via this process.

Bio-renewable liquid fuels are becoming more popular in recent years. This is mainly due to fuel price upsurges and environmental concerns. Bio-renewable liquid fuels can be plant based or animal based. Animal based liquid fuel comes from livestock fats. For example, REG Geismar, LLC, a fuel company located in Geismar, LA, has worked with

Tyson Foods in the last few years to convert animal fats to liquid fuels, which were then used or tested in vehicles and airplanes (Hulen, 2014). In the United States, ethanol, which is produced via corn fermentation, is one of the popular bio-liquid fuel products. Most of the gasoline that is used in vehicles contains up to 10% ethanol. U.S. fuel ethanol production has increased seven times in ten years, from 2,140 million gallons in 2004 to 14,300 million gallons in 2014 (RFA, 2015). Totally, non-crude liquid fuel consumption accounts for about 14% of the total liquid fuel usage in 2010 and this number is expected increase to 17% in 2040 (U.S. EIA, 2015).

Alga is one of the potential candidates for biofuel production. Growing algae for biofuel production is not a new concept. Back in 1978, the U.S. Department of Energy's Office of Fuels Development already funded programs to develop algae biofuel. However, the studies showed a high production cost was the main obstacle to this process at the time (Sheehan et al., 1998). With increasing fuel price over the past decade, many energy companies have started to develop a process to convert algae to biofuel. Algae biofuel is now commercially available. Algenol, a biofuel company in Florida, has commercially-produced algae bio-fuel at around $1.30 per gallon at production levels of 8,000 total gallons of liquid fuel per acre per year (Gorman, 2014).

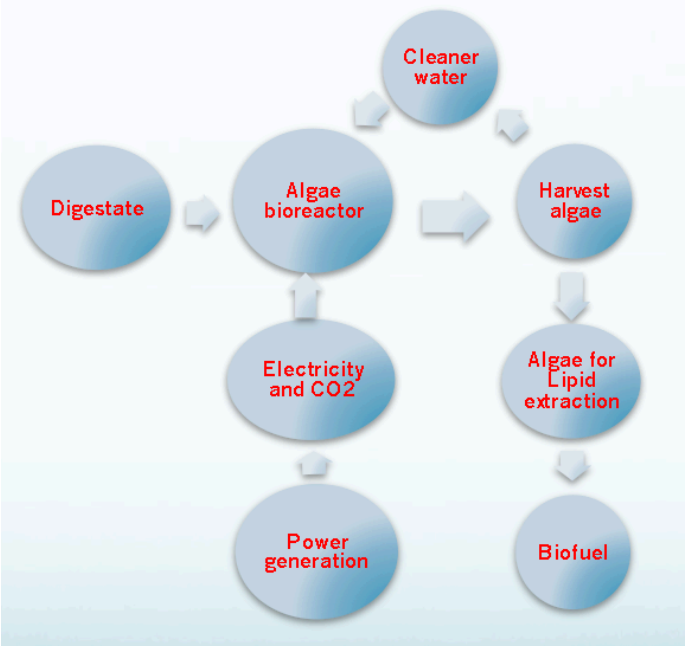

Figure 1.1: A way to use digestate and wasted carbon dioxide emission to grow algae for biofuel.

One method for reducing productions costs is by combining algae production with waste treatment. Digestate is the remaining substance after anaerobic digestion of a biodegradable feedstock, such as livestock manure. It is rich in inorganic contents, which makes it a good candidate for growing algae and making algae-based biofuel more affordable. Figure 1.1 illustrates a possible and economical way to use digestate to grow algae. Algae growth uses the inorganic contents in digestate, plus water, carbon dioxide from a source such as power plant emissions, and either natural light or electric lights, plus electricity for machine operation. After the algae are harvested, cleaner water could be recycled back to use in growing algae again. The lipids would be extracted from the algae to make biofuel. This process would reduce the nutrients in digestate that could cause a harmful impact on the environment if released. In addition, it would reduce the cost to grow algae and reduce carbon dioxide emissions to the environment.

The main objective of this study is to identify the digestate (*D*), magnesium sulfate ($MgSO_4$) and dipotassium hydrogen phosphate/potassium dihydrogen phosphate (*K-P*) concentrations that would optimize the algae growth. A previous study by a master's student had showed digestate at around 1.25% to 1.75% (v/v) dilution was the optimal concentration that would maximize algae growth rate and lipid concentration (Schwenk, 2010). However, according to the manufacturer's data and our measurements (shown in Table III), many essential inorganic nutrients for algae growth are relatively low in 1% digestate dilution, such as phosphorus and magnesium. As a result, $MgSO_4$ and *K-P* were added to the diluted digestate growth media with the intention that this supplementation may either increase growth rate, maximum biomass concentration, or both.

In many studies of algae growth in batch reactors, the specific growth rate (u_g) is reported as a parameter to define the algae growth during the exponential phase in many studies. To reduce subjectivity of defining the exponential phase while utilizing all the experimental data, a nonlinear four-parameter logistic regression equation was used to curve fit the experimental data to better define the algae growth by estimating two algae growth parameters: the maximum growth rate (r) and the maximum algae concentration (X_{max}). In addition, two more quantitative parameters, such as average biomass productivity (P_a) and instantaneous biomass productivity (P_i) are estimated and compared. The significance of each of these five algae growth parameters will be more clarified in the Background chapter.

To reach the main objective of this study, a central composite design method was used to design the test matrixes. From the measured data, response surface regression

equations were generated for each of the algae growth parameters: r, X_{max}, P_a, P_i, and u_g, and the optimal D, $MgSO_4$, and K-P concentrations for algae growth were then identified.

The first experimental set (Experiment 1) was focused on studying the effects of digestate, $MgSO_4$, and a wider range of K-P concentration on algae growth. The second experimental set (Experiment 2) was designed to study the effects of $MgSO_4$ and K-P at constant digestate concentration and to explore lowest concentration boundaries of these two factors, where no $MgSO_4$ and K-P was added.

Differences in the growth parameters were observed between Experiments 1 and 2. To identify possible experimental errors, data from four center point runs are compared in this study.

CHAPTER II

BACKGROUND

2.1 Algae Species

Scenedesmus dimorphus, is a type of fresh water microalga. As shown in Figure 1, it is a single cell alga in elongate shape; it could grow individually and also in groups. There are several reasons why this species had been chosen for this study. For instance, *Scenedesmus dimorphus* is able to survive in harsh environments. *Scenedesmus obliquus* (another name *for S. dimorphus*) is able to survive in a range of temperature, from 10 to 25 ^{o}C, with herbicide atrazine added. The algae growth rate did not show much effect by the herbicide atrazine (Chalifour & Juneau, 2011). In addition, *Scenedesmus obliquus* could grow in three different types of waste discharge, and the results showed that it still contained desirable fatty acid profile for biodiesel production (Mandal & Mallick, 2011). Wastewater is similar to diluted digestate in water, which might indicate that *Scenedesmus dimorphus* is suitable to grow in a digestate environment as well.

Other reasons for using this species are because of its fast growth rate, adequate fatty acid profile to produce biodiesel, and high biomass and lipid productivities. With studying different strains of *Scenedesmus obliquus*, Yang's research group had found two strains with growth rates higher than 1.0 day^{-1}, while the least growth rate was 0.6 day^{-1}

(Yang et al. 2011). In another study, *Scenedesmus obliquus* is found to have the most adequate fatty acid profile to produce biodiesel, namely in terms of linolenic and other polyunsaturated fatty acids (Gouveia & Oliveira, 2009). Higher lipid contents also make *Scenedesmus* a good candidate for biofuel production. A study by Mandal's group had showed *Scenedesmus obliquus* could have lipid accumulation up to 43% of the dry biomass under nitrogen deficiency growth conditions (Mandal & Mallick, 2009). Other than this, the biomass and lipid productivities for *Scenedesmus sp.* were high i.e., 217.50 and 20.65 mg $L^{-1}d^{-1}$ respectively when compared to *B. Brauni* with 26.55 and 5.51 mg $L^{-1}d^{-1}$ (Yoo et al. 2009).

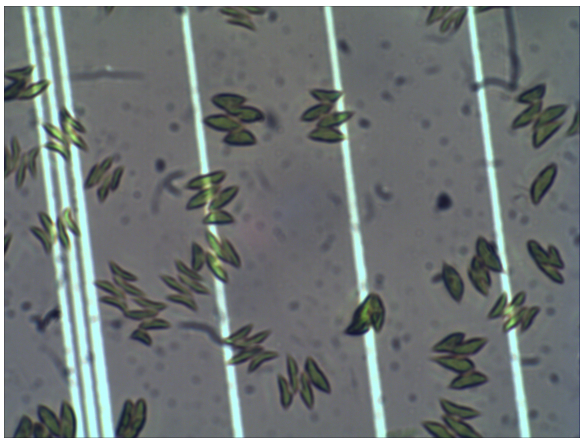

Figure 2.1: *Scenedesmus dimorphus* algae cells under 40X microscope.

Similar to many other single cell organisms, the growth curve of *Scenedesmus dimorphus* also follows four different growth phases in a batch reactor, as drawn in Figure 2.2. At the very beginning, there is a lag phase. When the algae cells are first inoculated into the reactor, it requires some time to adapt to the new environment. After that, it goes through the exponential growth phase. As the algae cells are about to use up the nutrients in the reactor or reaching the reactor carrying capacity, or become light or

CO_2 limited, the growth rate slow down, and the algae cells reach stationary phase. Finally, given enough time, the algae cells begin to die off during death phase.

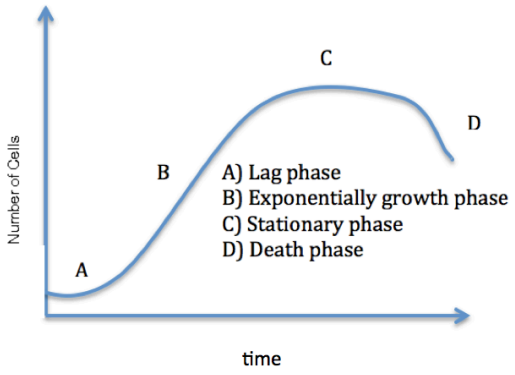

Figure 2.2: Four different growth phases of algae cells in batch reactor vs. time.

2.2 Digestate

Digestate is the byproduct of the livestock manure that had undergone anaerobic digestion. The process from which would remove most of the organic contents but leave rich inorganic contents. Figure 3.1 shows diluted digestate in water that was used in this study. Most of the solid particles had filtered out by centrifugation. However, at high concentration (e.g. 20% v/v dilution), the diluted digestate might not be suitable to grow algae because it causes a decrease in light penetration through the growth media. A previous study showed digestate at about 1.25% to 1.75% (v/v) dilution was the optimal concentration that would maximize algae growth and lipid concentration (Schwenk, 2010). As shown on the right picture of Figure 3.1 digestate growth media becomes clearer at a low concentration (2% or less dilution).

According to manufacturer's data as listed on Table III, 1% (v/v) dilution of digestate in water contains 25% of the nitrogen and 0.83% of the phosphorus used in 3N-BB media, a recommended algae media that is used in laboratories. Nitrogen and phosphorus are two

main nutrients required for algae growth. If the European Union uses algae biofuels for all their transportation need, this would require about 25 million tons nitrogen and 4 million tons phosphorus per year (Wijffels and Barbosa, 2010). Saving of these nutrients that are required for growing algae would lower the cost of biofuel production. On the other side, reducing the effluents of digestate to rivers or lakes might reduce the chance of algae bloom. As the results, many reports or studies have focused on using algae to reducing levels of nitrogen, and phosphorus in digestate or livestock manure effluents from daily farms. For example, Franchino-Marta's group showed algae could reduce nitrogen content by 90% and phosphorous content by 80% from digestate (Franchino et al., 2013).

Growing *Scenedesmus sp.* was found to be better when swine manure digestate was diluted in lake water (Bjornsson et al. 2013). Lake water might contain other minerals that were missing in digestate for growing algae. Other nutrients that were found to help growing algae in digestate were iron (Bchir et al., 2011).

There is often a trade-off between growth rate and final biomass production. Another study showed increasing the digestate and initial algae concentration might reduce the growth rate of algae while increasing the biomass production rate (Uggetti, et al. 2014).

2.3 Magnesium Sulfate

Magnesium is a main component in the chlorophyll structure in algae. One molecule of chlorophyll contains one molecule of magnesium (Bollivar, 1997). Photosynthetic plants or algae require chlorophyll for light or energy up taking. Little study has yet to be done on the magnesium sulfate effect on algae growth. One former study in 1939 showed high magnesium sulfate concentration is required for cell multiplication, while

magnesium sulfate deficiency would lead to increase in cell size (Trelease & Selsam, 1939). High levels of magnesium sulfate may help maintain high chlorophyll content in algae, which may promote cell division and growth.

A former M.S. student also found that magnesium sulfate concentration at half 3N-BB media level (about 3.5 mg/L) or above would have similar algae growth rate (Schwenk, 2010). Another study showed magnesium might not have much effect on algae growth with addition of swine manure digestate (Bjornsson et al., 2013). The reason could possibly be due to the swine manure digestate was diluted with lake water, which may contain high enough level of magnesium than required to grow algae.

2.4 Dipotassium Hydrogen Phosphate/Potassium Dihydrogen Phosphate

One reason for using the combination of dipotassium hydrogen phosphate and potassium dihydrogen phosphate is for pH control. The ratio of dipotassium hydrogen phosphate to potassium dihydrogen phosphate uses in this study is 1 to 3. The resulted pH is about 6.4 (pK= 6.86 at 25 ^{o}C) (DeAngelis, 2007). Due to the risk of contamination, pH was not measured or monitored in this study.

Phosphorous is an important nutrient for algae growth, and it has been found to be a main component in algae cells. The empirical formula for microalgae is $C_{106}H_{263}O_{110}N_{16}P$, which means nitrogen to phosphrous ratio is of 7.2 to 1 mass ratio. According to a study, the nitrigen to phosphorous mass removal ratio by algae was around 5:1 to 8:1 when both elements were abundant in the growth media (Li et al. 2010). This ratio could be significantly different when algae grow in harsh environement. For *Scenedesmus obliquus* growing in piggery wastewater, the algae removed 155 mg total nitrogen and 4 mg total phosphorous per gram of dried algae for growth (Ji et al. 2013). The N/P mass

ratio in this case was about 39 to 1.

Algae might be able to grow at low phosphorous environments. An earlier study had showed the phosphorous level could be reduced to (5.3mg/L of phosphorous) 1/10 of the 3N-BB media level without adversely affecting growth or lipid productivity (Welter et al. 2013).

Different phosphorous concentrations in the growth media may cause differences in cell size and algae lipid contents. Chen's research group in China showed high phosphorous contents at 25 ^{o}C would give higher chlorophyll content in algae but smaller algae cell sizes (Chen et al., 2011). High phosphorous content here means 10 mg/L. Furthermore, nitrogen depletion and phosphorous repletion might give higher lipid production in algae (Li et al., 2010). Many other studies also showed similar results. For example, *Scenedesmus dimorphus* in nitrogen starvation had raised up to 24.2% of lipid production while at normal condition was about 11% (Xu et al., 2015). In another case, lipid accumulation in *Scenedesmus obliquus* was studied under various culture conditions. The lipid production could reach 43% of dry cell weight (under N-deficiency) while it was about 12.7% under control condition (Mandal & Mallick, 2009).

2.5 Algae Growth Assessment Methods

Algae growth rate is an important parameter in studying algae. The algae growth rate that had been reported in the literatures was ranging from 0.1 to 2.89 day^{-1} (Xu and Boeing 2014; Zhang, et al., 2009). The algae growth rate assessment methods depend on the algae growth theories. A popular method to assess the algae growth rate is the exponential phase growth rate assessment. This method assumes the algae growth rate is constant at the exponential phase, and the change in algae concentration is defined as:

Equation 2.1:

$$\frac{dX}{dt} = u_{net}X$$

for which dX/dt = change in algae concentration, X = algae concentration at a given time, and u_{net} = the net specific growth rate. When the cell death rate is relatively insignificant during exponential growth phase, the net specific growth rate is equal to the specific growth rate (u_g) (Shuler and Kargi, 2002).

By integrating Equation 2.1, the specific growth rate (u_g) is defined as the slope of the following equation:

Equation 2.2:

$$\ln(X_e) = u_g(t_e - t_b) + \ln(X_b)$$

where X_e and X_b are the ending and beginning algae concentration of the exponential growth phase, and t_e and t_b are the ending and beginning time of the exponential growth phase. The ending and beginning of the exponential growth phase could be estimated by two ways. One is the "visual inspection" method; this method contains subjective errors. By plotting the logarithm of the algae concentration vs. time, the ending and beginning of the exponential growth phase are determined by the experimenter (Anjos et al. 2013). Another way is to start the experiment with a short lag phase and end the experiment before the end of the exponential growth phase. X_b would then be the initial concentration and X_e would be the ending concentration (Gu et al. 2012).

Another method to assess the algae growth rate is the logistic growth model. This model assumes the algae growth rate (u) at any given point of the algae growth curve depends on a maximum growth rate (r), the algae concentration at the time (X), and the

maximum algae concentration (X_{max}) that could reach as shown in Equation 2.3 (Shuler & Kargi, 2002).

Equation 2.3:

$$u = r\left(1 - \frac{X}{X_{max}}\right)$$

This equation has used in "Droop" model, the classical algae growth model built by M. *R*. Droop in the 1960s (Lemesle & Mailleret, 2008). The use of this model in analyzing experimental data is not common. It mostly was used in modeling the algae growth in different nutrient or environmental conditions (Mailleret et al., 2005). For example, JinShui Yang's group used this model with experimental data to assess the growth of algae, *Chlorela Minutissima*, and its lipid production under photoheterotrophic fermentation conditions (Yang et al., 2011). The results showed that model predictions agreed with experimental data. Another study had used the logistic growth model to assess the algae growth rate and biomass production of on growing *Scenedesmus sp.*, under both phosphorous-starvation and nutrient rich cultivation conditions (Wu et al., 2012). This study found algae grew under phosphorous-starvation condition would give better biomass productions.

By substituting Equation 2.3 into Equation 2.1 and integrating the combined equation, the algae concentration at a given time (X) could be calculated with a four-parameter logistic equation as shown in Equation 2.4 (Details integration is in Appendix A).

Equation 2.4:

$$X = X_{min} + \frac{X_{max} - X_{min}}{1 + e^{-r\,(t - t_{50})}}$$

The four parameters are maximum algae concentration (X_{max}), maximum growth rate (r), minimum algae concentration (X_{min}), and time for algae concentration to reach 50% of X_{max} (t_{50}).

With known *X, r, and* X_{max}, two more quantitative parameters could be calculated: Average biomass productivity (P_a) and instantaneous biomass productivity (P_i). For growing algae in batch reactor, it is time consuming to run the reactor to reach the X_{max}. The batch reactor might be more economically feasible to stop once the average biomass productivity (P_a) drops significantly. The average biomass productivity is defined as:

Equation 2.5:

$$\mathrm{P}_a = \frac{\Delta X}{\Delta t} = \frac{X_{max} \times f}{t_f}$$

Where, f = fraction, any number between 0% to 100%; P_a =average biomass productivity over the time period from inoculation to the time when the biomass concentration (X) reaches the fraction (f) of X_{max}; t_f =time required for X to reach that fraction (f) of X_{max}. The time t_f is calculated by setting X *equal to* fX_{max} in Eq. 2.4, and rearranging to yield:

Equation 2.6:

$$t_f = t_{50} - \frac{e^{\left(\frac{X_{max}-X_{min}}{fXmax-X_{min}}-1\right)}}{r}$$

While running a CSTR reactor at steady state, the optimal dilution rate (D) is equal to the growth rate, and the reactor biomass productivity is calculated as the dilution rate times the biomass concentration in the CSTR reactor (Shuler & Kargi, 2002). As shown in Figure 2.2, each given point on the growth curve has an instantaneous biomass productivity (P_i) since the algae biomass concentration and algae growth rate vary at any

given point. Calculating this instantaneous biomass productivity might help define the maximum biomass productivity while growing algae in the CSTR reactor. The instantaneous biomass productivity at each point along each growth curve could be estimated with the following equation,

Equation 2.7:

$$\text{instantaneous } biomass\ productivity\ (P_i) = uX$$

where *X* is the algae cell concentration and u is the algae growth rate at a given time in the reactor.

With the four-parameter logistic equation, the instantaneous biomass productivity at each given point along the growth curve is estimated from the following equation:

Equation 2.8:

$$P_i = r\left(1 - \frac{X}{X_{max}}\right)X$$

2.6 Absorbance and Cell Numbers

UV-vis spectrophotometric optical density or absorbance is a way to measure the algae concentration without counting cells under microscope. Absorbance at 600nm is a common absorbance value to measure the biomass and cell count. Studies showed algae concentration has a linear relationship with absorbance at an absorbance value below one, and this linear relationship failed at absorbance values greater one (Myers et al., 2013). The absorbance method applies Beer's law, which is defined as:

Equation 2.9:

$$A = \log\left(\frac{I_o}{I}\right) = \alpha Lc$$

for which A is the absorbance, I_o is the intensity of the light incident on the sample, I is the intensity of the light transmits through the sample, α is the absorption coefficient of the sample, and L is the path length (O'Haver, 2015). Concentration is a logarithm function of the ratio of I_o over I. At high concentration, light transmitting through the sample becomes less sensitive to concentration changes. Transmittance measurement errors increase, which results inaccuracy in the absorbance readings. As shown in the dilution curve in Figure 2.3, the linearity of the algae sample in 1.5% digestate solution changes at about 0.9 of the absorbance value.

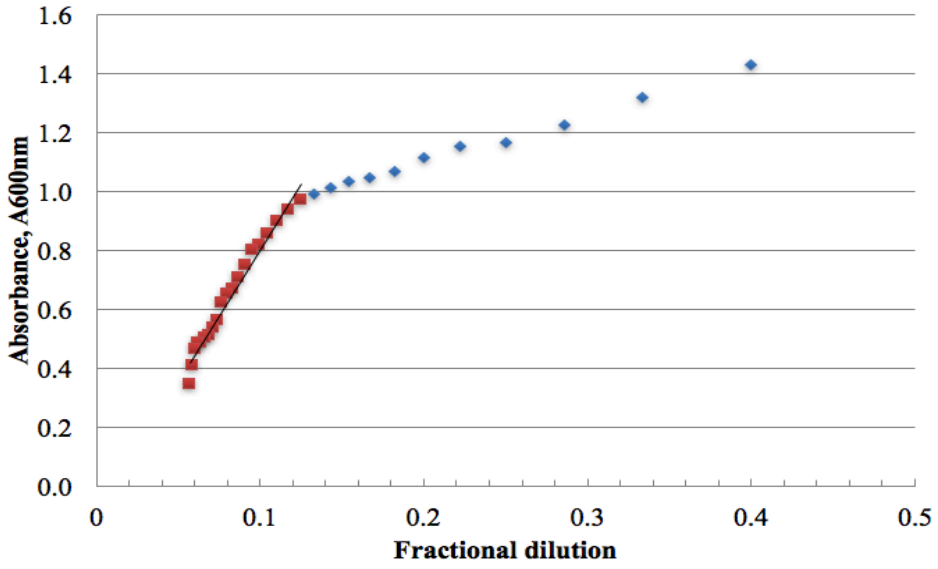

Figure 2.3: Absorbance vs. fractional dilution of algae after growing in 1.5% v/v digestate solution (data obtained by Satya Girish Avula).

The shape and contents of the algae might affect the absorbance as well. The cell number and absorbance relationship are linear for many types of algae. However, the slope of the line is different for different types of algae (Held and Banks, 2012). For *S. Dimorphus*, a former Master's thesis study confirmed the linear relationship between the biomass concentrations and the absorbance reading at 600 nm, with the slope of the line

equal to 0.5 gdw/L/A_{600} (Kanani, 2013). As the result, A_{600} reading was used to measure the algae concentrations in this study. For algae sample with absorbance value of 0.9 or above, the sample was diluted, and the adjusted absorbance value was reported instead.

2.7 Central Composite Design

To define the concentration of the three factors that would result the optimum of the algae growth parameters while reducing numbers of experimental points, the central composite design was selected for this study. With three factors (*D*, $MgSO_4$, and *K-P*), the central composite design space is spherical, which means all the points are equidistant from the center and prediction variances were equal for all the points (Myers and Montgomery, 2009). The design test matrix should contain eight corner points, six axial points, and at least five center points. As shown on Figure 2.4, the corner points were at the eight corners of the cube and touching the surface of the sphere, and axial points were on the axis lines and touching the sphere surface. The center points were at the center of the cube and center of the sphere. With this experimental design, response surface regression equations were generated for the response variables: maximum algae concentration (X_{max}), average biomass productivity (P_a), maximum growth rate (r), instantaneous biomass productivity (DX) and specific growth rate (u_g), in the format as shown as Equation 2.10, which is a function of linear, quadratic, and interactive effective terms of the factors (digestate, magnesium sulfate, dipotassium hydrogen phosphate/potassium dihydrogen phosphate).

Equation 2.10:

$$X_{max}, P_a, \mathrm{u}_g, P_i, \ or\ r = C_1 + C_2D + C_3MgSO_4 + C_4KP + C_5D^2 + C_6(MgSO_4)^2 + C_7(KP)^2 + C_8D(MgSO_4) + C_9D(KP) + C_{10}MgSO_4(KP)$$

where C_1 to C_{10} are the coefficients for each effective term of the factors, D is percentage of digestate dilution (v/v), $MgSO_4$ is magnesium sulfate concentration (mmole), and K-P is the concentration of dipotassium hydrogen phosphate/potassium dihydrogen phosphate (mmole).

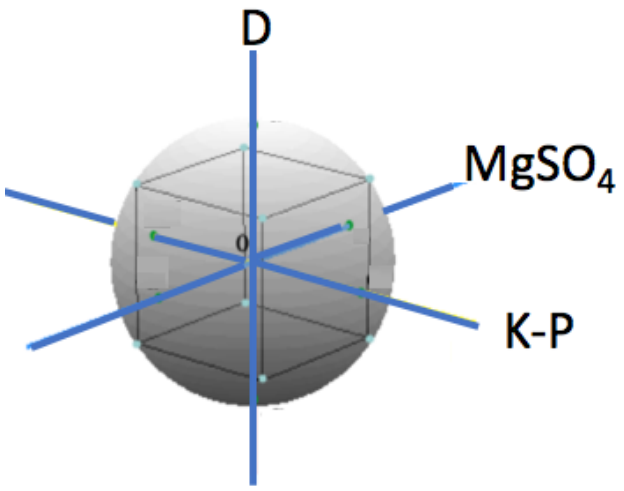

Figure 2.4: Central composite design in three-dimensional space.

2.8 Induced Coupled Plasma Spectroscopy

Induced coupled plasma spectroscopy is an analytical technique that use to measure the elemental concentrations in a solution. The ICP spectroscopy involved vaporizing the sample to its elemental components with inductively coupled plasma. The individual elements emit visible light at a specific wavelength. The intensities of light emissions are then translated as the elemental concentrations. The elemental concentrations are linearly related to light emission intensity for up to four to six order magnitudes (Hou and Jones, 2000). The measurement process starts with calibrations by measuring solutions with

known elemental concentrations. Then, an ICP measurement on an unknown solution would determines its elemental concentrations.

ICP spectroscopy can be used to measure most naturally occurring elements, except hydrogen, oxygen, fluorine, and inert gases (Hou and Jones, 2000). Nitrogen, an important element for algae growth, is hard to be precisely measured due to high background effects caused by the atmospheric nitrogen (Almeida et al., 2005). Other than that, most elements are commonly occurring in compound form with other elements, such as phosphorus (P) in phosphate (PO_4) or phosphite (PO_3). The ICP measurements would not be able to determine which compound does the element comes from.

CHAPTER III

MATERIALS AND METHODS

3.1 20% (v/v) Digestate Solution Preparation

Digestate was obtained from GHD, Inc. in Chilton, WI. The original digestate solution contained solid particles and liquid. The digestate was first diluted to 20% (v/v) with D.I. water in 50 ml centrifuge tubes (each tube contained 10 ml digestate and 40 ml of D.I. water). Each tube was shaken well and then centrifuged at 1000 rpm for 20 min at room temperature. After centrifugation, the solid particles were discarded.

3.2 Digestate Samples Preparations for Elemental Concentration Measurements

The elemental concentrations were measured in digestate samples by means of Induced Coupled Plasma (ICP) spectroscopy. Six digestate samples (10 ml each) were withdrawn from the digestate container. The container bracket was shaken well between each withdrawal. The digestate in each tube was diluted down to 20% (v/v) in water, and solids removed, as described in Section 3.1. Each of the six 20% (v/v) supernatants was further diluted into either 0.5%, 1.0%, or 1.5 % (v/v) with D.I. water. The final diluted digestate solutions (each with volume = 150 mL) then were autoclaved at "Liquid for 250 ML" setting. The cycle took about 1 hour and 15 minutes. After autoclaving, 9 ml

autoclaved D.I. water was added to each sample to compensate for evaporative losses under autoclaving. Then, the samples were readied for ICP measurements. The pictures on Figure 3.1 shows the 20% and 0.5 to 1.5% diluted digestate solutions. ICP measurements were performed by Dereck Johnson in Analytical Chemistry Lab, NASA Glenn Research Center.

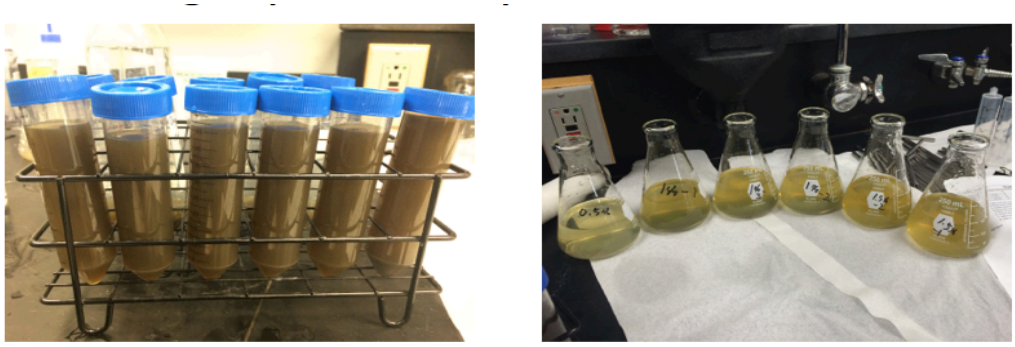

20% v/v digestate 0.5 to 1.5 % digestate

Figure 3.1: 20% and 0.5 to 1.5 % v/v diluted digestate solution in D.I. water.

3.3 Algae Sources and Inoculation

Scenedesmus dimorphus was obtained from the UTEX culture collection (ID# 746 Austin, TX). Algae cells were maintained in agar. For inoculation, small amount of algae cells in agar were scraped from agar and placed into a 2 liter bottle that contained modified triple nitrate Bold's Basal (3N-BB) media, which had 0.75g $NaNO_3$, 0.025 g $CaCl_2*2H_2O$, 0.075 g $MgSO_4*7H_2O$, 0.075 g K_2HPO_4, 0.175 g KH_2PO_4, and 0.025 g NaCl per 1 liter of D.I. water and 6 mL trace metal stock solution containing 0.75 g/L Na_2EDTA, 0.097 g/L $FeCl_3*6H_2O$, 0.041 g/L $MnCl_2*4H_2O$, 0.005 g/L $ZnCl_2$, 0.002 g/L $CoCl_2$, and 0.004 g/L $NaMoO_4$. All these chemicals were brought from Sigma –Aldrich Cor. The inoculation bottle was enclosed by a rubber stopper (Figure 3.2c) that had three tubes passed through. Air contained 5% CO_2 flowed through one tube at a flow rate of

0.1 LPM. The inoculation bottle was placed on top of a stir plate at room temperature. A magnetic stir bar was placed inside the bottle to keep the algae cells well-mixed in the growth media. Six 14 watt, 48" Accupro fluorescent tubes were used to provide illumination on a 12 hours on/12 hours off cycle.

3.4 Algae Growth Media

Magnesium sulfate stock solution was prepared by adding 1.5 g of $MgSO_4$ in 200 ml of D.I. water. The K_2HPO_4 stock solution was prepared by adding 1.5 g of K_2HPO_4 in 200 ml of D.I. water, and KH_2PO_4 stock solution was prepared by adding 3.5 g of KH_2PO_4 in 200 ml of D.I. water. The resulting concentrations for these three are respectively 0.0305M, 0.0431M, and 0.129M.

The algae growth media contained digestate, magnesium sulfate and/or dipotassium hydrogen phosphate/potassium dihydrogen phosphate. The total working volume for each algae growth media was 150 ml. 20% diluted digestate solution, stock solutions, and D.I. water were added to 250 mL Ehrlenmeyer flasks, at amounts needed to achieve the concentration shown in Table I and Table II. Equal volumes of K_2HPO_4 stock solution and KH_2PO_4 stock solution were added to the algae growth media, to achieve the total phosphate concentrations specified. The flasks were then covered with aluminum foil and autoclaved on the cycle designated as "liq 250 mL 121.0^{o}C S = 0:30:00". The cycle took about 1 hour and 15 minutes. After autoclaving, the growth media was cooled down to room temperature in a laminar airflow sterile hood. Immediately after, 9 ml autoclaved D.I. water and a volume of algae suspension from the prepared inoculum were added to each flask. The volume of the inoculum was calculated using Equation 3.1.

Equation 3.1:

$$(0\times150) + (V_r\times A_i) = 0.1\times(V_r + 150)$$

for which, V_r is the volume of the inoculum needed, A_i is the absorbance volume (A600) of the inoculum, 150 is the total working volume of the algae growth media, 0.1 is the desired starting absorbance (A600) value of the algae growth media after adding the algae cells.

3.5 Algae Growth Experimental Set Up

The experiments were conducted at Cleveland State University, Room 405. Algae cells were grown in growth media in 250 mL flasks that contained different amounts of *D*, *$MgSO_4$*, and *K-P* as listed in Table I and Table II. The total volume of each growth media was 150 mL. Eight flasks were grouped into one block and were run at the same time in a shaker water bath as shown in Figure 3.2 b. The flasks were randomly rotated in position within the shaker bath once per day. The shaker rotated at about 150 rpm to help maintain the algae and nutrients well-mixed in the growth media. The water bath was set at a constant temperature of 30 ^{o}C. Seven florescent tubes were hung on top of the shaker water bath as show in Figure 3.2a, to provide illumination on a 12 hours on/12 hours off cycle. These seven florescent tubes were three Bulbrite T5 fluorescent tubes (14 Watts and 3,000K) alternated with four CoraLife high output aquarium T5 tubes (24 watt and 10,000K). The height of the tubes was adjusted to give light intensity of 550 to 600 foot-candles over the metal-plate that held the flasks.

Each 250 mL flask was closed by rubber stopper as shown in Figure 3.2c. The rubber stopper and tubing were autoclaved at 121 ^{o}C before used. Three tubes were inserted through the stopper. One tube was for air and CO_2 mixture inlet gas. A sterile 2 um syringe filter was placed at the inlet of the tubing to filter and eliminate possible contamination in the air and CO_2 mixture. Shop air was used and mixed with CO_2 (from CO_2 bottle, CD50) at 95 to 5 volumetric ratios before entering the flask. The flow rate was controlled by rotameter at 0.1 LPM. Another tube was the aseptic sampling port,

which was designed to withdraw algae sample for absorbance measurement. Before entering the flask, two tubes were joined by a T-connector. One tube was for sample withdraws, while another with syringe filter was for air that was used to clear out any liquid left in the sampling tube before and after sampling. The third tube was for the gas vent. One end of the tubing was placed in the headspace of the flask, while another end was open to the atmosphere. Cotton was placed in the tubing to prevent bacteria from entering into the flask.

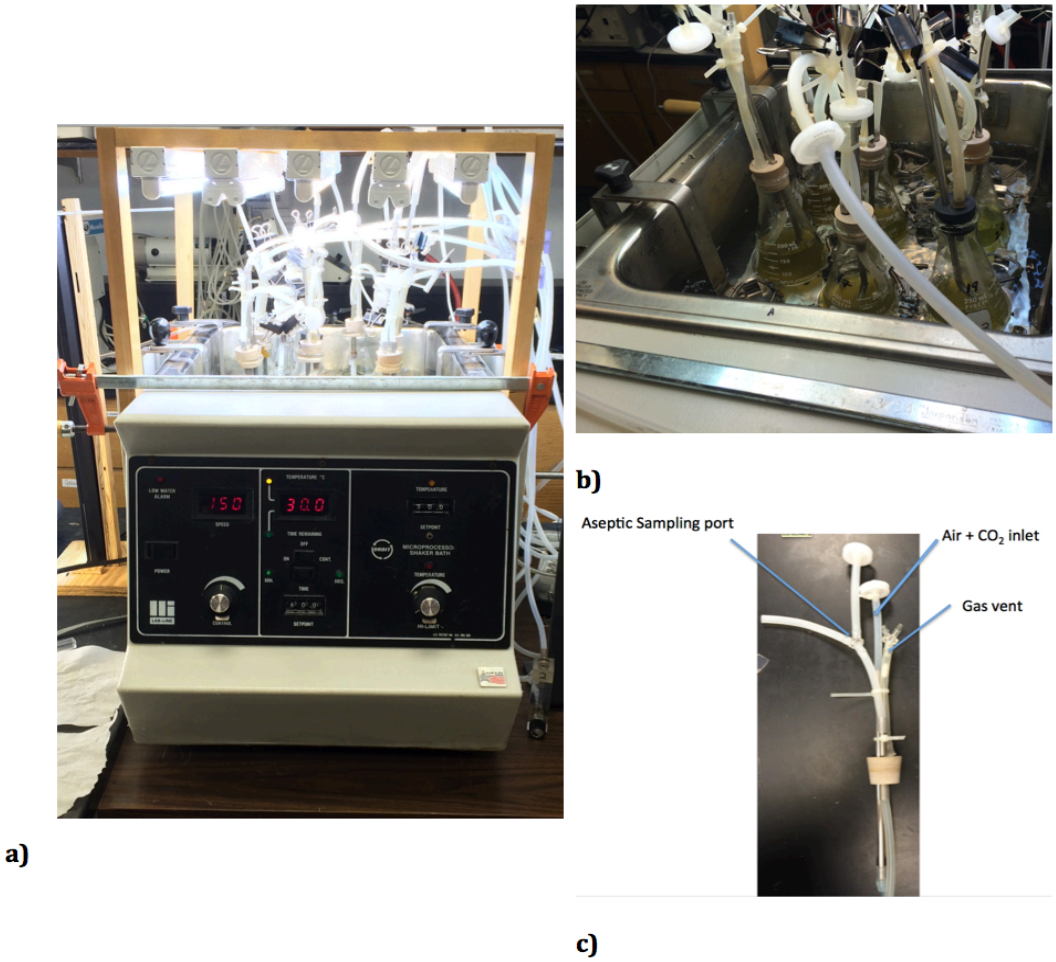

Figure 3.2: a) water bath, b) algae batch reactors experimental setup, and c) aseptic sampling tubing for each batch reactor.

3.6 Daily Sampling Procedure

The algae culture was sampled one hour after set-up and once each day for twelve consecutive days. About 2 ml of algae culture was withdrawn every time to measure absorbance at 600 nm. 2 ml of autoclaved D.I. water was added to the algae culture to account for loss in evaporation each day. Before and after sampling, 30% ethanol solutions were spread over the hand and tubing to eliminate contaminations. Fisher Scientific™ Traceable™ Dual-Range Light Meter was used to measure light intensity every four days.

Optical density or absorbance was measured at 600 nm using Genesys 10S UV-Vis spectrophotometer. Algae cells scatter most of the light at wavelength of 600 nm, which have found to be a consistent wavelength for determining cell concentration (Held, 2011). D.I. water was used as blank. If the reading was higher than 0.9, the algae sample was diluted accordingly. To obtain the final adjusted absorbance reading, the absorbance of the sample was subtracted by the absorbance of a media sample (without algae) with the same digestate concentration. Absorbance values for each run were taken daily for 12 to 13 days.

Orflo MOXI Z mini automated cell counter was used to assess cell size distribution in Experiment 2, block 3 and 4. The cell size measurements were performed in day 4 and day 8 of Experiment 2. 0.75 uL of each algae sample was used each time.

3.7 Calculation and Estimation Methods for the Algae Growth Parameters: u_g, X_{max}, r, P_a, and P_i

The specific growth rate (u_g) was obtained by plotting natural log of algae concentration (X) vs. time (t), and calculating as the slope of the exponential phase as shown by Equation 2.1. Figure 3.3 is an example for estimating u_g. A linear curve is

fitted through the exponential growth phase, which is from day 1 to day 5 for this data, and the slope of the line is the specific growth rate. The experimenter determines the beginning and ending day of the exponential growth phase by visual inspection.

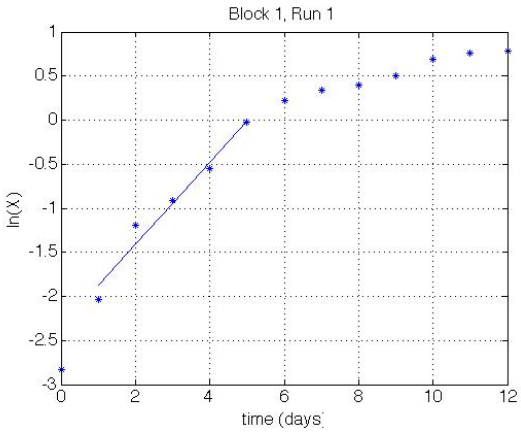

Figure 3.3: Natural log of X plotted against time to determine u_g.

Many integrated forms of the logistic equation are available. To better fit the experimental data, the maximum algae concentration (X_{max}), the maximum growth rate (r), the minimum algae concentration (X_{min}), and the time for algae concentration to reach 50% of X_{max} (t_{50}) for each batch reactor were estimated by the nonlinear fitting of the experimental absorbance data with the four-parameter logistic equation (Equation 2.4) in Minitab Version 17. Average biomass productivity (P_a) and instantaneous biomass productivity (P_i) were calculated with Equation 2.5 and Equation 2.8 respective.

3.8 Design Models and Test Matrices for Experiment 1 and Experiment 2

Table I shows the design test matrix for Experiment 1. There were twenty-four runs of growth media. Each growth media contained different concentrations of digestate, magnesium sulfate, and potassium hydrogen phosphate. The coded values of each factor were ranged from -1.633 to +1.633. The digestate concentrations ranged from 0.184% to

1.817% (v/v) dilution. The concentration magnesium sulfate and *K-P* in each growth media was varied between 0.112 to 1.108 mmole/L, and 0 to 5.619 mmole/L respectively.

The test matrix was divided into three blocks due to experimental facility limitation. The experimental set-up could only handle eight runs at a time. Ten center points were distributed among the three blocks, which helped connecting this central composite design together. Within each block, the coded values for each factor added up to zero. This indicated the design was orthogonal, which meant the estimations on the coefficients were independent of each other. Experimenter, Satya Girish Avula, preformed and collected absorbance data for all three blocks of Experiment 1.

The author conducted Experiment 2. Experiment 2 only studied the various levels of magnesium sulfate and potassium hydrogen phosphate while digestate was at 0.83% (v/v) dilution in all flasks. The test matrix is listed in Table II. Totally, there were thirty-two runs divided into four blocks. No center points were included in the first two blocks. There were two replicates for each of the eight edge points on the designed blue rectangle as shown on Figure 3.2. The second two blocks contained eight center points and one each of the eight edge points. Blocks 1 and 2 were run at same time in different shakers, and Blocks 3 and 4 were run at same time in different shakers after that.

Figure 3.4 compares the experimental design spaces for Experiment 1 and Experiment 2. Experiment 1 covers broader concentration range of *K-P*, while Experiment 2 covers broader concentration range of $MgSO_4$. The center of the Experiment 2 rectangle had shifted to lower concentrations of magnesium sulfate and potassium hydrogen phosphate.

Response surface regression equations for the response variables were generated by using the backward elimination method with alpha value set at 0.1 with Minitab software.

When a p-value of an effective term in the equation was higher than 0.1, the corresponding term was considered not significantly different from zero and removed from the equation. The terms were hierarchical. A quadratic term was higher than interaction term, and then linear term. When a higher order term of a factor was significant, a lower order term of that factor would also be kept in the equation even if its effect was not significant.

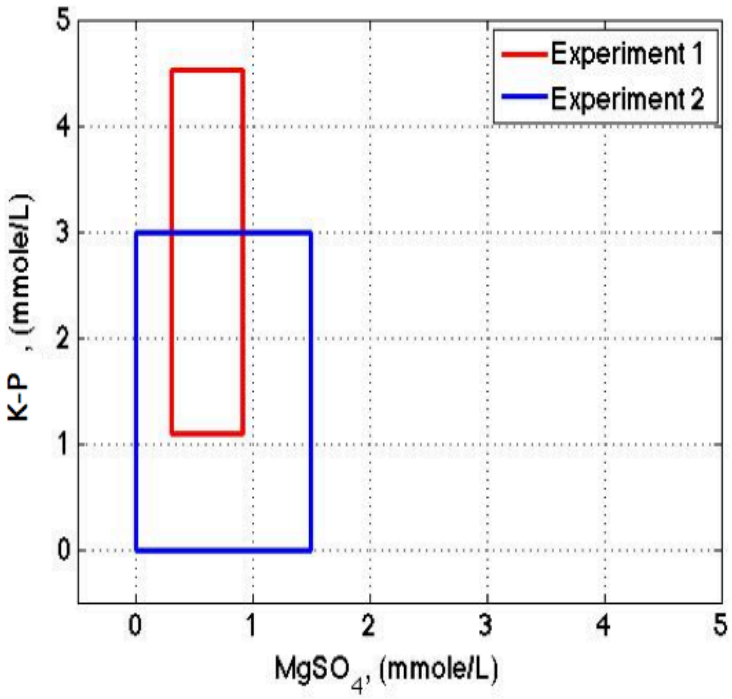

Figure 3.4: Experiment 1 and 2 design spaces for *$MgSO_4$* and *K-P*.

Table I: Experiment 1 design test matrix, amounts of *$MgSO_4$*, *K-P*, and digestate in each growth media.

Block	**Run**	**$MgSO_4$ coded**	***K-P* Coded**	***D* coded**	**$MgSO_4$ (mmole/L)**	***K-P* (mmole/L of PO_4)**	***D* (%, v/v)**
1	1	1	-1	1	0.915	1.09	1.5
1	2	0	0	0	0.61	2.81	1
1	3	0	0	0	0.61	2.81	1
1	4	0	0	0	0.61	2.81	1
1	5	-1	-1	-1	0.305	1.09	0.5
1	6	1	1	-1	0.915	4.53	0.5
1	7	0	0	0	0.61	2.81	1
1	8	-1	1	1	0.305	4.53	1.5
2	1	0	0	0	0.61	2.81	1
2	2	-1	1	-1	0.305	4.53	0.5
2	3	0	0	0	0.61	2.81	1
2	4	1	-1	-1	0.915	1.09	0.5
2	5	1	1	1	0.915	4.53	1.5
2	6	-1	-1	1	0.305	1.09	1.5
2	7	0	0	0	0.61	2.81	1
2	8	0	0	0	0.61	2.81	1
3	1	0	0	0	0.61	2.81	1
3	2	0	-1.633	0	0.61	0	1
3	3	0	1.633	0	0.61	5.619	1
3	4	0	0	-1.633	0.61	2.81	0.184
3	5	-1.633	0	0	0.112	2.81	1
3	6	0	0	1.633	0.61	2.81	1.817
3	7	1.633	0	0	1.108	2.81	1
3	8	0	0	0	0.61	2.81	1

Table II: Experiment 2 design test matrix, amounts of *$MgSO_4$*, *K-P*, and digestate in each growth media.

BLOCK	Run	$MgSO_4$ coded	*K-P* Coded	MgSO4 (mmole/L)	*K-P* (mmole/L of PO_4)	*D* (%, v/v)
1	1	-1	1	0	3	0.83
1	2	-1	-1	0	0	0.83
1	3	1	1	1.5	3	0.83
1	4	1	-1	1.5	0	0.83
1	5	-1	1	0	3	0.83
1	6	-1	-1	0	0	0.83
1	7	1	1	1.5	3	0.83
1	8	1	-1	1.5	0	0.83
2	1	-1	0	0	1.5	0.83
2	2	0	1	0.75	3	0.83
2	3	0	-1	0.75	0	0.83
2	4	1	0	1.5	1.5	0.83
2	5	-1	0	0	1.5	0.83
2	6	0	1	0.75	3	0.83
2	7	0	-1	0.75	0	0.83
2	8	1	0	1.5	1.5	0.83
3	1	0	0	0.75	1.5	0.83
3	2	1	1	1.5	3	0.83
3	3	1	-1	1.5	0	0.83
3	4	-1	1	0	3	0.83
3	5	0	0	0.75	1.5	0.83
3	6	-1	-1	0	0	0.83
3	7	0	0	0.75	1.5	0.83
3	8	0	0	0.75	1.5	0.83
4	1	0	0	0.75	1.5	0.83
4	2	0	0	0.75	1.5	0.83
4	3	0	1	0.75	3	0.83
4	4	0	0	0.75	1.5	0.83
4	5	1	0	1.5	1.5	0.83
4	6	0	0	0.75	1.5	0.83
4	7	-1	0	0	1.5	0.83
4	8	0	-1	0.75	0	0.83

CHAPTER IV

RESULTS AND DISCUSSION

4.1. Digestate Elemental Concentrations and Homogeneity Analysis (ICP-MS data)

Inductively Coupled Plasma Mass Spectrometry (ICP-MS) was used to determine the elemental concentration of Ca, K, Mg, Na, P, and S in six of the diluted digestate samples, in order to assess homogeneity of the original digestate slurry and compare its composition to that of laboratory media. Each of these samples was diluted from six individual digestate slurry samples taken from the same original digestate container. The dilutions were varied from 0.5% to 1.5% (v/v) in D.I. water. Table III lists the elemental concentrations in each of these diluted digestate samples. The data shows the concentrations of each elements in the diluted digestate solutions are closely related to the degree of the dilutions. This verifies the homogeneity of the original digestate and the consistency of the method that was used to prepare the diluted digestate growth media.

Table IV compares the average ICP-MS elemental measurements for the diluted digestate at 1% (v/v) (n=3) to the digestate manufacturer's data at 1% and the 3N-BB media. Concentrations determined by ICP-MS for all elements are lower than the manufacturer's data, especially for K and P, which are respectively about 1/10 and 1/5 of

manufacturer's data. Some of the elements might be removed from the diluted digestate solutions along with the solid particles during the centrifugation process. Moreover, the manufacturer may have done the measurements from a very large, perhaps poorly mixed, volume from which the 5-gal sample was removed and shipped to CSU.

Nitrogen, phosphorous, potassium, and magnesium are essential for algae growth. Nitrogen concentration cannot be determined with the ICP-MS technique. According to manufacturer's data, 1% diluted digestate (v/v) contained about 32 mg/L of elemental nitrogen, which is about 1/4 that of the 3N-BB media. The concentrations in the 1% diluted digestate (ICP-MS data) of magnesium, potassium, and phosphorous are respectively about 1/2, 1/10 and 1/50 that of the 3N-BB media.

Table III: Elemental compositions of diluted digestate in water, ICP-MS data.

% digestate	Ca	K	Mg	Na	P	S
	mg/L	mg/L	mg/L	mg/L	mg/L	mg/L
0.5%	0.62	6.2	1.33	3.7	0.4	0.6
1.0%	1.51	13.3	3.25	7.5	0.8	1.1
1.0%	1.55	13.1	3.24	7.4	0.8	1.2
1.0%	1.65	13.3	3.31	7.6	0.8	1.2
1.5%	2.54	18.9	4.78	11.1	1.1	1.7
1.5%	2.45	19.1	4.83	11.1	1.1	1.6

Table IV: Elemental compositions of 1%-diluted digestate in water, ICP-MS data vs. digestate manufacture data vs. 3N-BB media.

	Ca	K	Mg	Na	P	S	N
	mg/L	mg/L	mg/L	mg/L	mg/L	mg/L	mg/L
Average 1% digestate (ICP-MS data)	1.57 (n=3)	13.23 (n=3)	3.27 (n=3)	7.50 (n=3)	0.80 (n=3)	1.17 (n=3)	
Standard deviation	0.07	0.12	0.04	0.10	0.00	0.06	
1 % digestate (manufacture data)	2.20	131.00	5.60	8.40	4.40		32.00
3N-BBM	7.00	118.00	7.00	213.00	53.00	9.80	124.00

4.2 Four-Parameter Logistic Equation Non-linear Regressions

The daily absorbance data for each run was fitted with the four-parameter logistic equation by using the non-linear regression method in Minitab 17 (Figures 4.1 and 4.2). For Experiment 1 block 3 run 4, only the first eight absorbance readings were used in the non-linear regression due to the death phase that was observed after day 9. The X_{min}, X_{max}, r, and t_{50} values for each run in Experiment 1 and Experiment 2 are listed in Table V and Table VI, and curve fits and experimental data for each run are plotted in Figure 4.1 and Figure 4.1

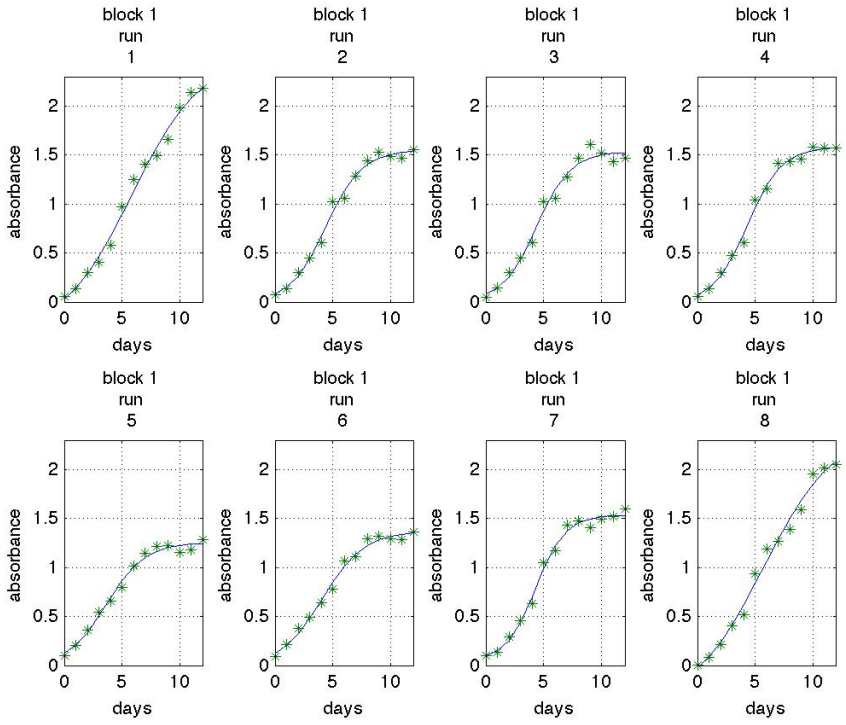

a) Experiment 1, Block 1

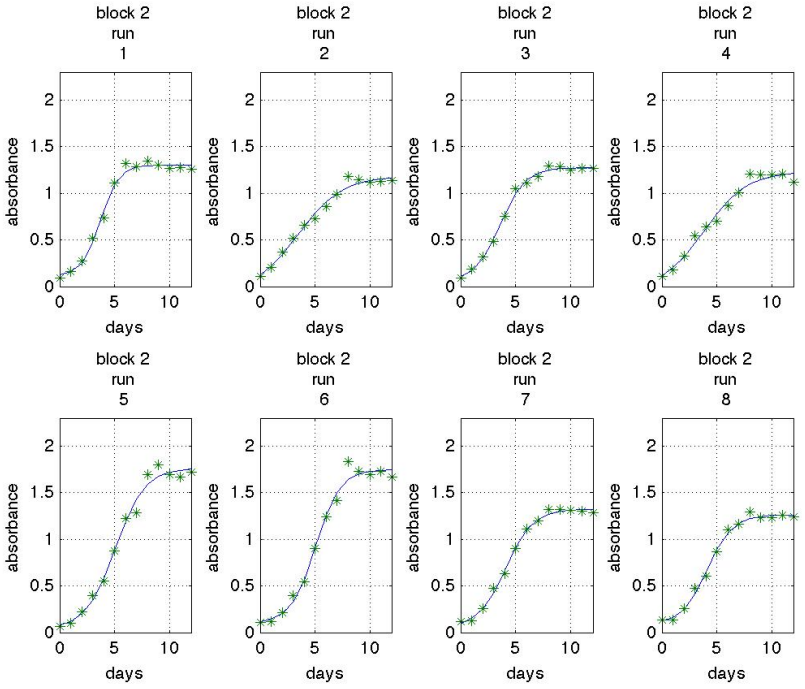

b) Experiment 1, Block 2

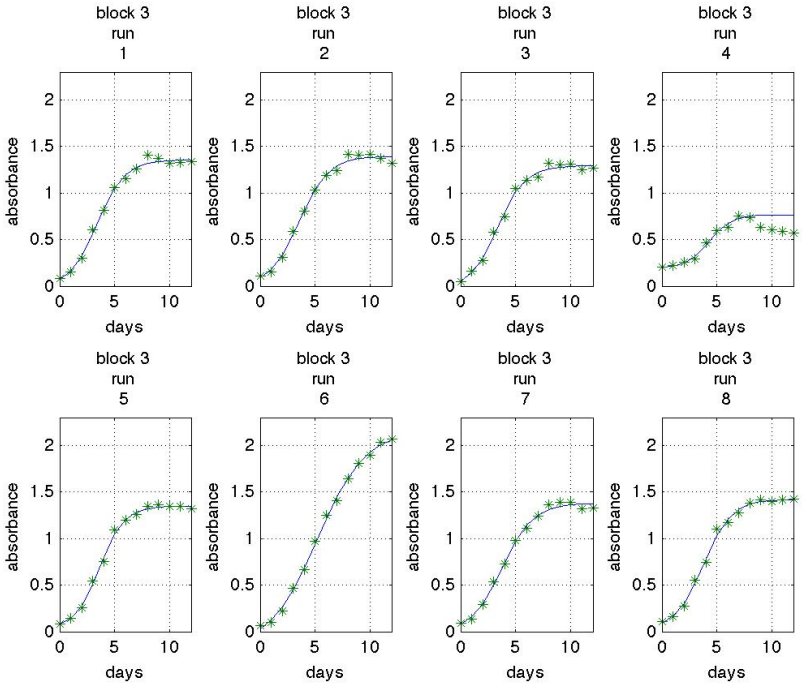

c) Experiment 1, Block 3

Figure 4.1: Absorbance data (*) and curve fits for Experiment 1, a) Block 1, b) Block 2, and c) Block 3 (Last four data points of Block 3 Run 4 were not used in curve fitting. This set of experimental data were collected by Avula (Avula, 2016).

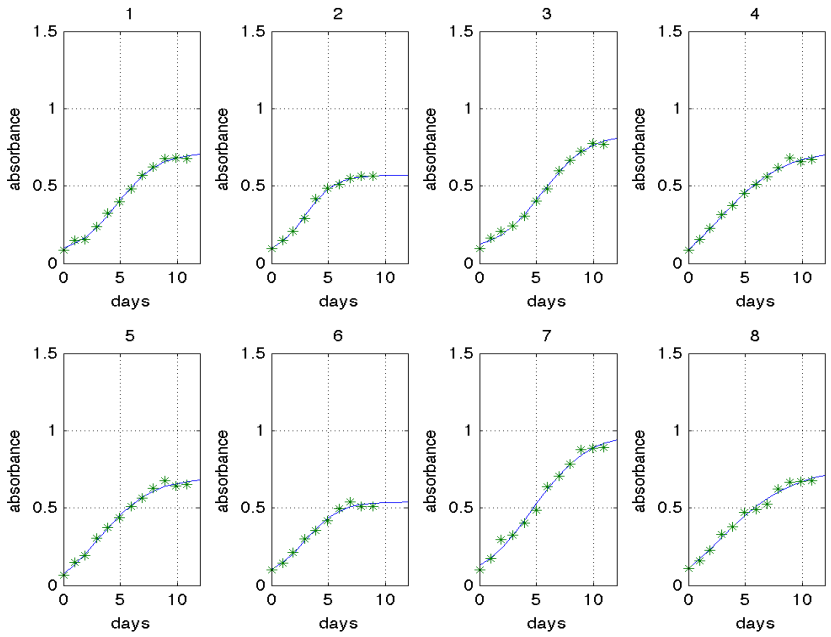

a) Experiment 2, Block 1

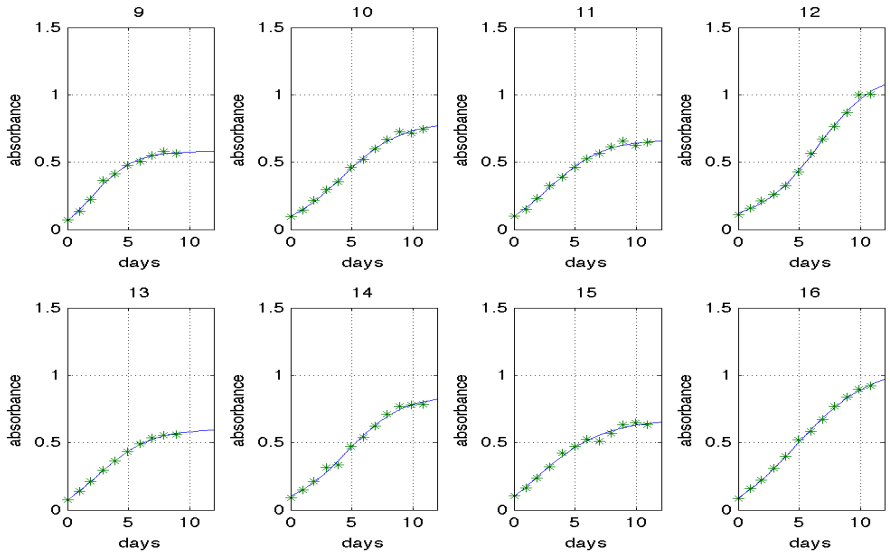

b) Experiment 2, Block 2

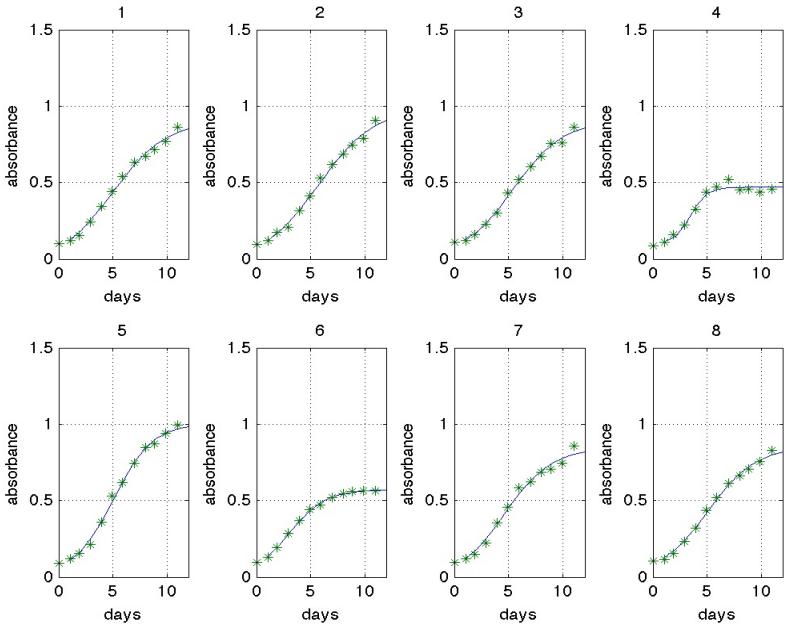

c) Experiment 2, Block 3

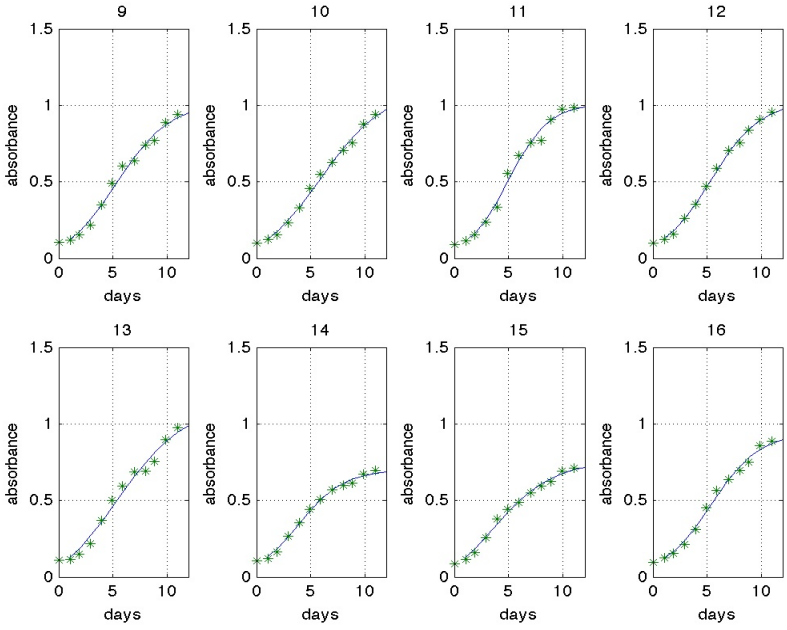

d) Experiment 2, Block 4

Figure 4.2: Experiment 2 absorbance data (*) and curve fits, a) Block 1, b) Block 2, c) Block 3, d) Block 4.

Table V: Experiment 1 X_{min}, X_{max}, r, t_{50}, P_{a90}, $P_{i\max}$, and u_g. (Standard errors list in APPENDIX B)

Block	MgSO4 coded	K-P Coded	*D* coded	X_{min}	X_{max}	r	t_{50}	P_{a90}	$P_{i\max}$	u_g
1	1	-1	1	-0.349	2.531	0.327	5.835	0.181	0.206	0.466
1	0	0	0	-0.006	1.547	0.641	4.398	0.178	0.244	0.467
1	0	0	0	0.005	1.533	0.681	4.377	0.181	0.257	0.463
1	0	0	0	-0.01	1.578	0.676	4.312	0.188	0.263	0.479
1	-1	-1	-1	-0.014	1.254	0.587	3.623	0.153	0.182	0.384
1	1	1	-1	0.003	1.368	0.558	4.117	0.153	0.191	0.315
1	0	0	0	0.055	1.534	0.79	4.326	0.194	0.301	0.488
1	-1	1	1	-0.425	2.421	0.32	5.705	0.173	0.193	0.57
2	0	0	0	0.112	1.305	1.197	3.701	0.212	0.366	0.483
2	-1	1	-1	-0.08	1.186	0.488	3.404	0.135	0.144	0.383
2	0	0	0	0.057	1.276	0.869	3.6	0.187	0.266	0.435
2	1	-1	-1	-0.044	1.235	0.506	3.803	0.136	0.156	0.429
2	1	1	1	0.042	1.761	0.744	5.06	0.198	0.328	0.527
2	-1	-1	1	0.103	1.746	0.901	5.046	0.21	0.393	0.507
2	0	0	0	0.059	1.322	0.814	4.096	0.175	0.269	0.489
2	0	0	0	0.091	1.262	0.867	4.117	0.171	0.274	0.462
3	0	0	0	-0.021	1.356	0.78	3.387	0.197	0.257	0.58
3	0	-1.633	0	0	1.393	0.747	3.557	0.193	0.253	0.561
3	0	1.633	0	-0.034	1.294	0.795	3.352	0.19	0.25	0.479
3	0	0	-1.633	0.193	0.765	0.979	4.26	0.106	0.182	0.359
3	-1.633	0	0	0.032	1.346	0.91	3.631	0.2	0.296	0.516
3	0	0	1.633	-0.176	2.161	0.456	5.195	0.194	0.243	0.569
3	1.633	0	0	-0.007	1.376	0.721	3.761	0.182	0.246	0.485
3	0	0	0	0.021	1.419	0.778	3.769	0.194	0.273	0.483

Table VI: Experiment 2 X_{min}, X_{max}, r, t_{50}, P_{a90}, $P_{i\max}$, and u_g (Standard errors list in APPENDIX B)

BLOCK	$MgSO_4$ coded	K-P Coded	X_{min}	X_{max}	r	t_{50}	P_{a90}	$P_{i\max}$	u_g
1	-1	1	0.053	0.716	0.554	4.711	0.076	0.099	0.271
1	-1	-1	0.057	0.570	0.798	2.994	0.092	0.113	0.342
1	1	0	0.076	0.836	0.504	5.480	0.078	0.105	0.220
1	1	-1	-0.153	0.733	0.356	2.742	0.069	0.065	0.299
1	-1	1	-0.083	0.696	0.437	3.144	0.074	0.076	0.281
1	-1	-1	0.048	0.539	0.682	3.005	0.080	0.092	0.303
1	1	0	-0.002	0.987	0.413	4.633	0.089	0.102	0.234
1	1	-1	-0.198	0.764	0.303	2.559	0.065	0.058	0.301
2	-1	-1	-0.107	0.583	0.580	1.922	0.087	0.085	0.389
2	0	1	-0.025	0.799	0.418	4.155	0.076	0.083	0.300
2	0	-1	-0.050	0.669	0.461	2.895	0.077	0.077	0.319
2	1	1	0.055	1.178	0.423	6.505	0.092	0.124	0.240
2	-1	-1	-0.093	0.600	0.467	2.430	0.072	0.070	0.323
2	0	1	0.002	0.853	0.441	4.549	0.081	0.094	0.284
2	0	-1	-0.246	0.676	0.347	1.497	0.069	0.059	0.317
2	1	1	-0.123	1.067	0.328	4.635	0.082	0.087	0.298
3	0	0	-0.038	0.904	0.400	4.938	0.077	0.090	0.351
3	1	1	-0.016	0.987	0.390	5.718	0.078	0.096	0.313
3	1	-1	0.025	0.898	0.453	5.459	0.079	0.102	0.326
3	-1	1	0.097	0.469	1.367	3.448	0.087	0.160	0.371
3	0	0	0.022	1.006	0.560	5.100	0.101	0.141	0.398
3	-1	-1	0.009	0.572	0.601	3.048	0.077	0.086	0.356
3	0	0	-0.010	0.844	0.474	4.655	0.082	0.100	0.361
3	0	0	0.007	0.853	0.453	5.067	0.078	0.097	0.347
4	0	0	-0.039	1.018	0.401	5.283	0.084	0.102	0.371
4	0	0	-0.074	1.109	0.331	5.854	0.079	0.092	0.348
4	0	1	0.009	1.010	0.545	4.973	0.101	0.138	0.376
4	0	0	-0.007	1.025	0.440	5.316	0.089	0.113	0.356
4	1	0	-0.125	1.124	0.317	5.364	0.080	0.089	0.395
4	0	0	-0.006	0.698	0.486	3.931	0.074	0.085	0.389
4	-1	0	-0.136	0.758	0.357	3.490	0.067	0.068	0.417
4	0	-1	0.001	0.942	0.450	5.349	0.083	0.106	0.341

4.3. Average Biomass Productivity (P_a), Instantaneous Biomass Productivity (P_i), and Specific growth rate (u_g)

For algae growing in large-scale batch reactor mode, it might not be economical to run the process until reaching the maximum algae concentration. According to the logistic growth model of Equation 2.3 and 2.4 and experimental evidence in Figure 4.1 and 4.2, the rate of change in algae concentration increases at the beginning then decreases after passing time of t_{50}. As shown on Figure 4.3, maximum growth rate and maximum algae concentration for each run are weakly inversely related to each other. The run having higher growth rate did not necessary give higher or lower maximum algae concentration (X_{max}). Knowing both these properties might not indicate the optimal time at which the batch process should be stopped. The calculation of the average biomass productivity may help in this determination.

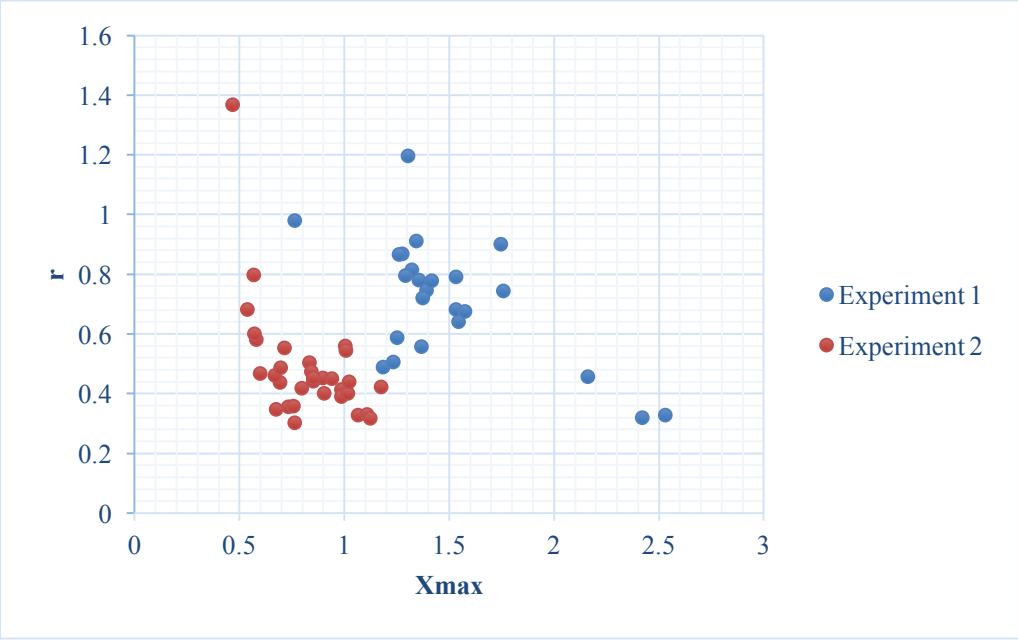

Figure 4.3: r vs. X_{max} for Experiment 1 and Experiment 2.

Average biomass productivity is defined as the fraction of X_{max} divided by the time (t_f) required to reach that fraction of X_{max} (given by f; Equation 2.5). The quantity t_f was calculated for each experimental run using Equation 2.6 for f between 0.40 and 0.99, using the parameters from Tables V and VI for r, t_{50}, X_{min}, and X_{max}. Figure 4.4 shows the average biomass productivity as a function of fraction of X_{max} for Experiment 1. The average biomass productivities were mostly increased or held steady until 0.80 to 0.90 of X_{max}, then dropped quickly as the algae concentration approached 90% of X_{max}.

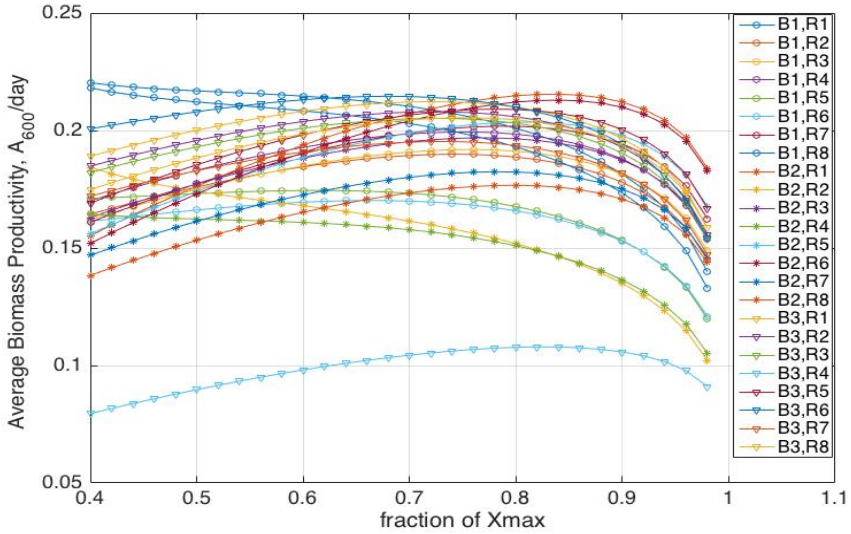

Figure 4.4: Experiment 1 average biomass productivity as a function of fraction of X_{max}.

Instantaneous biomass productivity (P_i) is related to algae concentration and growth rate at a given time. This quantity was calculated for each run, using the parameters from Tables V and VI for r, and X_{max}. By taking the derivative on of Equation 2.8,

Equation 4.1:

$$\frac{dP_i}{dX} = r(1 - \frac{2X}{X_{max}})$$

the maximum instantaneous biomass productivity ($P_{i\max}$) should occur at algae concentration of 50% of X_{max}. Figure 4.5 shows the instantaneous biomass productivity as

a function of fraction of X_{max} for Experiment 1. Each data point on these two graphs represents differences in algae biomass concentration at different nutrient concentrations, with resulting difference in algae growth rate. The algae growth rate is high due to high nutrient concentration at the beginning. However, the low algae concentration during that time diminishes the instantaneous biomass productivity. As the algae concentration increases overtime, the instantaneous biomass productivity increases until reaching 50% of X_{max}. After that, the algae concentration in the reactor reaches to a point where it approaches the maximum capacity of the reactor under the given conditions. The algae growth rate starts to decrease, which causes the instantaneous biomass productivity to decrease.

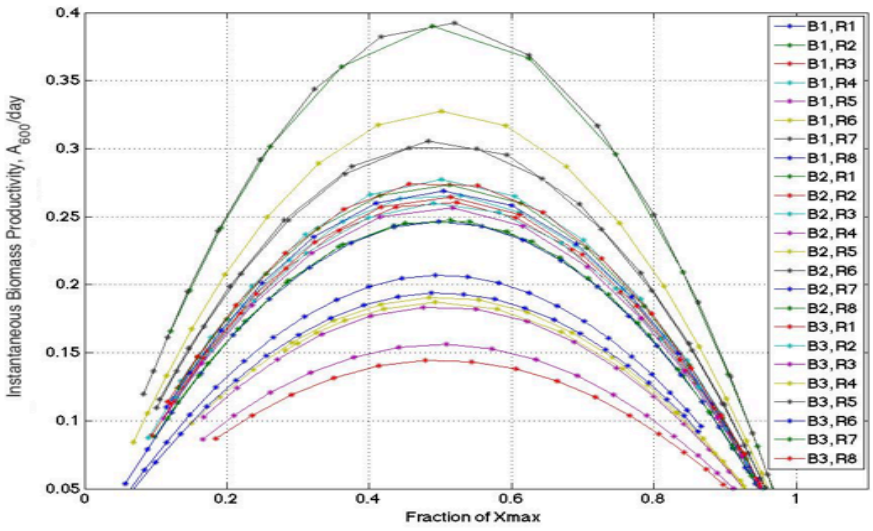

Figure 4.5: Experiment 1 instantaneous biomass productivity as a function of fraction of X_{max}.

Instead of P_a and P_i, this study will be focus on P_{a90}, the average biomass productivity as the algae concentration reaches 90% of X_{max}, and P_{imax}, the maximum instantaneous biomass productivity, which were calculated using:

Equation 4.2:

$$P_{a90} = \frac{0.9X_{max}}{t_{50} - e^{\left(\frac{X_{max}-X_{min}}{fX_{max}-X_{min}}-1\right)/r}}$$

Equation 4.3:

$$P_{imax} = \frac{rX_{max}}{4}$$

The specific growth rate (u_g) is the algae growth rate calculated during exponential growth phase, identified using the method of visual inspection, and using Equation 2.2. Figures 4.6 and 4.7 show the experimental data and curve fits across the exponential growth phase for Experiments 1 and 2, respectively. Values of specific growth rate for Experiment 1 and Experiment 2 are listed on Table V and Table VI. Due to the difference in digestate, $MgSO_4$ and *K-P* concentrations, the specific growth rate for Experiment 1 batches ranges 0.36 to 0.57 day^{-1}, while the specific growth rate for Experiment 2 batches ranges 0.22 to 0.39 day^{-1}.

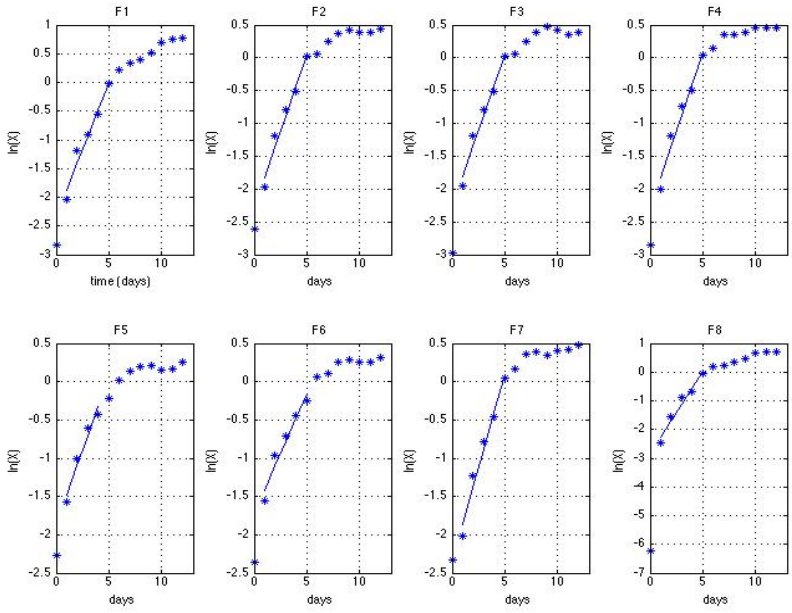

a) Experiment 1, Block 1

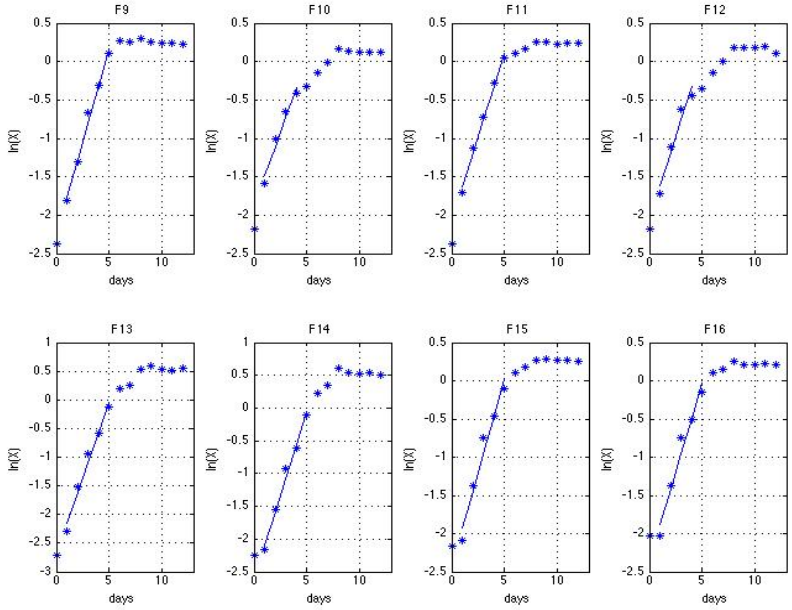

b) Experiment 1, Block 2

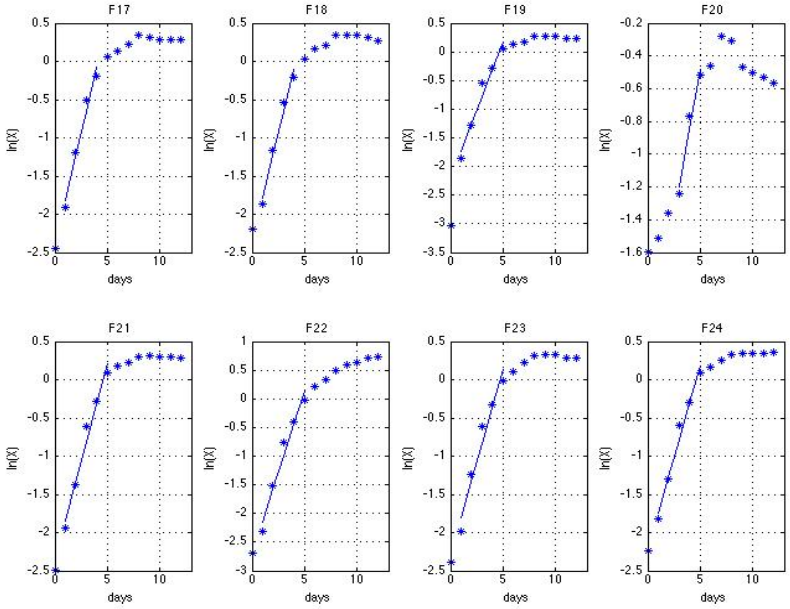

c) Experiment 1, Block 3

Figure 4.6: Experiment 1 absorbance data (*) and exponential growth phase curve fits for eight runs in a) Block 1, b) Block 2, and c) Block 3.

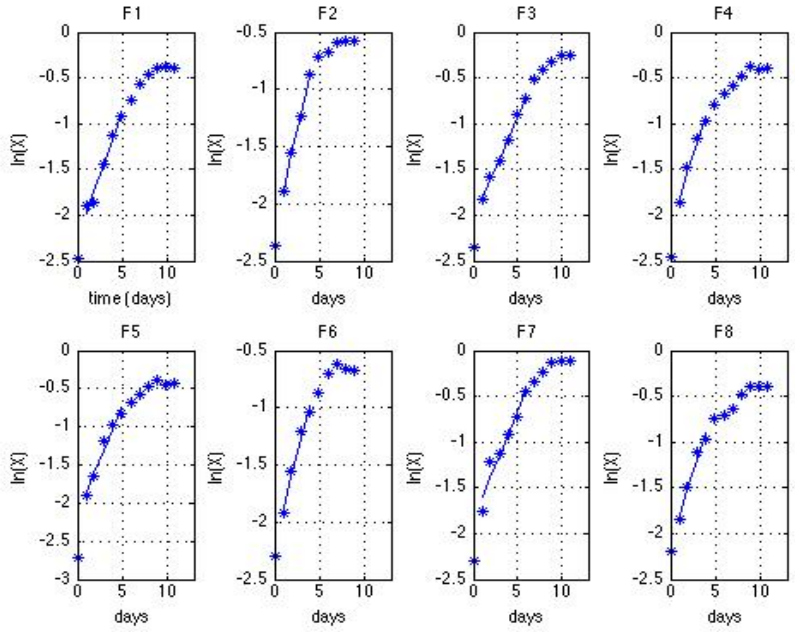

a) Experiment 2, Block 1

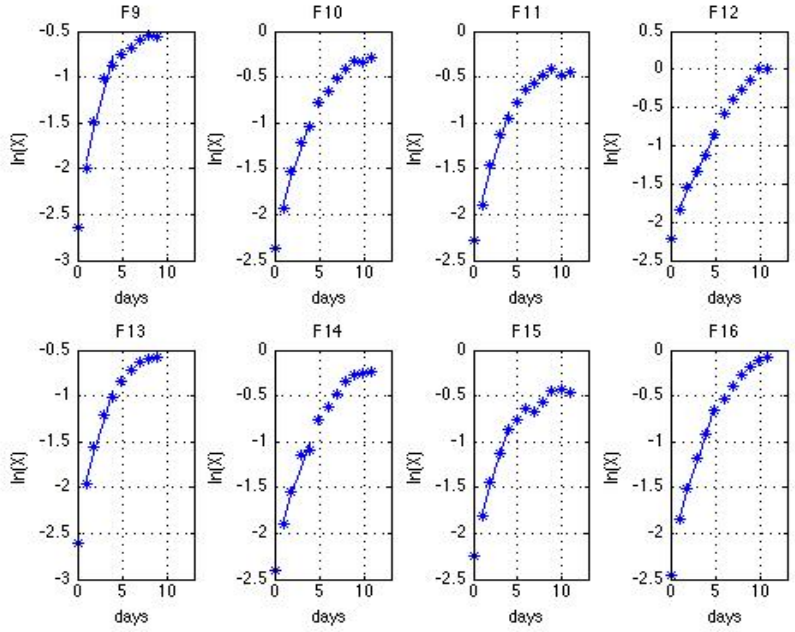

b) Experiment 2, Block 2

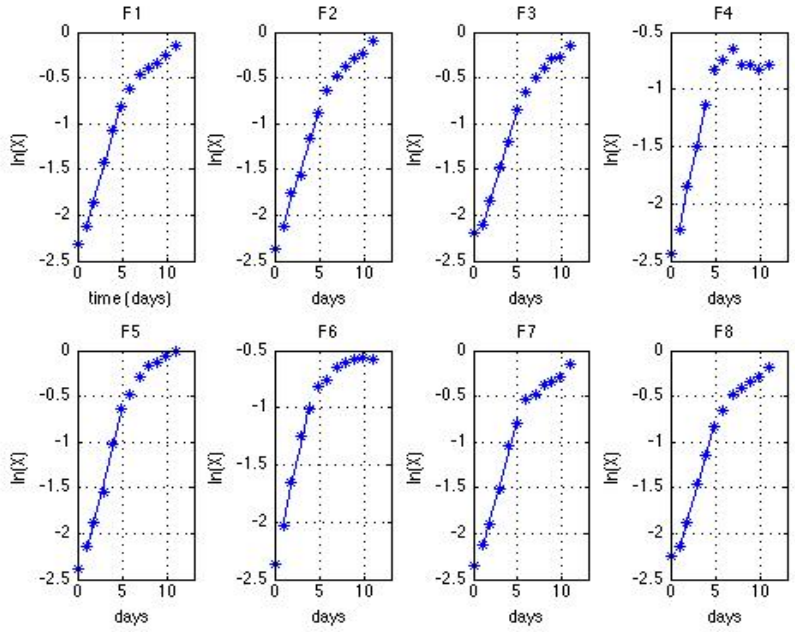

c) Experiment 2, Block 3

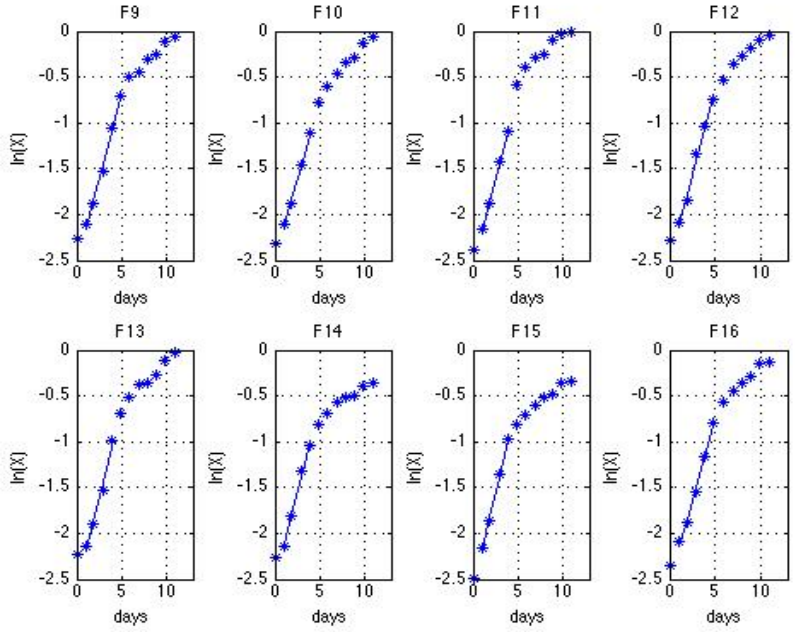

d) Experiment 2, Block 4

Figure 4.7: Experiment 2 absorbance data (*) and exponential growth phase curve fits for eight runs in a) Block 1, b) Block 2, c) Block 3, d) Block 4.

4.4. Response Surface Regression Equations for X_{max}, r, P_{a90}, $P_{i\max}$, and u_g

Using the data shown in Table I, Table II, Table V, and Table VI, response surface regression equations for the two experiments were generated for maximum growth rate (r), maximum algae concentration (X_{max}), average biomass productivity over the time period to the algae concentrations reaching 90% of X_{max} (P_{a90}), maximum instantaneous biomass productivity ($P_{i\max}$) and specific growth rate (u_g). The model equations were generated using linear regression with backward elimination with elimination alpha value set at 0.1 in Minitab 17. To maintain a balanced block design and better goodness of fit, all data points were used in the response surface regression equations. The data points with standardized errors greater than 2.0 were replaced by the model suggested fit values. Table VII and VIII list the coefficients and statistical parameters of the response surface regression equations.

The response surface regression equations for Experiment 1 shows good fits with the experimental data (($r^2 > 95\%$). The regression goodness of fit of X_{max} from Experiment 2 is high ($r^2 = 97.3\%$), but were lower for r, and u_g (r^2 between 73% to 89%). In addition, no regression equation could be generated for P_{a90} and $P_{i\max}$. These results might be caused by two reasons. First, Experiment 2 only tested the effect of $MgSO_4$ and K-P, and these two factors might not have strong effects on algae growth. Experimental errors were relatively larger for Experiment 2. Second, the regression equation may not be suitable to describe the effects of these two factors within the range that tested.

Table VII: Coefficients and corresponding statistical parameters of Experiment 1 Response Surface Regression equation for a) X_{max} and r, b) P_{a90}, $P_{i\max}$, and u_g vs. Block, D (v/v), $MgSO_4$ (mmole/L), and *K-P* (mmole/L). (C1 to C10 are the coefficients, as defined in Eq. 2.9)

a)

	X_{max}	P-values	r	P-values
C1	0.80±0.009	0.000	0.73±0.008	0.000
C2 (*D* (v/v))	0.014±0.0004	0.000	0.0±0.0	0.729
C3 ($MgSO_4$ (mmole/L))	0.05±0.01	0.175	-1.0+0.3	0.000
C4 (*K-P* (mmole/L))	0.06±0.03	0.112	-0.1±0.02	0.004
C5 (*D*^2)	0.4±0.05	0.000	-0.54±0.03	0.000
C6 ($MgSO_4$^2)	0.7±0.1	0.000		
C7 (*K-P*^2)	0.02±0.004	0.000	-0.014±0.003	0.000
C10 ($MgSO_4$ x *K-P*)	-0.3±0.03	0.000	0.3±0.02	0.000
R-square value	99.19%		98.14%	

b)

	P_{a90}	P-values	$P_{i\max}$	P-values	u_g	P-values
C1	0.118±0.001	0.000	0.293±0.003	0.000	0.384±0.002	0.000
C2 (*D* (v/v))	0.17±0.01	0.000	0.33±0.02	0.000	0.16±0.008	0.000
C3 ($MgSO_4$ (mmole/L))	-0.1±0.05	0.193	-0.4±0.08	0.001	0.03±0.007	0.002
C4 (*K-P* (mmole/L))	-0.01±0.01	0.293	-0.08±0.02	0.000	-0.03±0.01	0.018
C5 (*D*^2)	-0.06±0.007	0.000	-0.13±0.01	0.000	-0.06±0.01	0.000
C6 ($MgSO_4$^2)						
C7 (*K-P* ^2)						
C10 ($MgSO_4$ x *K-P*)	0.02±0.004	0.000	0.11±0.008	0.000	-0.025±0.003	0.009
C9 (*D* x *K-P*)					0.04±0.01	0.000
R-square value	95.07%		97.27%		97.28%	

Table VIII: Coefficients and corresponding statistical parameters of Experiment 2 Response Surface Regression equation for X_{max}, r, and u_g vs. Block, D (v/v), $MgSO_4$ (mmole/L), and *K-P* (mmole/L). (C1 to C10 are the coefficients, as defined in Eq. 2.9)

	X_{max}	P-values	r	P-values	u_g	P-values
C1	0.57±0.008	0.000	0.62±0.01	0.000	0.365±0.003	0.000
C2 (*D* (v/v))						
C3 ($MgSO_4$ (mmole/L))	0.34±0.02	0.000	-0.2±0.03	0.000	-0.03±0.005	0.000
C4 (*K-P* (mmole/L))	0.1±0.01	0.000	0.0±0.0	0.697	-0.01±0.003	0.000
C5 (*D*^2)						
C6 ($MgSO_4$^2)	-0.1±0.02					
C7 (*K-P*^2)	-0.02±0.006	0.043				
C10 ($MgSO_4$ *X K-P*)			0.05±0.01	0.000		
R-square value	97.3%		74.55%		88.64%	

4.5 Algae Cell Size and Cell Count Measurements

As observed under the microscope, the *Scenedesmus dimorphus* cell is 2 to 4 um wide and 5 to 7 um long. Assuming this algae cell is a cylinder tube with a dimeter of 2 to 4 um and 5 to 7 um long, the effective diameter, calculated with Equation 4.4:

Equation 4.4:

$$effective\ diameter = 2\left(cylinder\ volume\left(\frac{3}{4\pi}\right)\right)^{1/3}$$

ranges from 3.10 um to 5.52 um. The Orflo MOXI Z mini automated cell counter uses the Coulter Principle for cell number and cell size measurement, for which it gives an average volume reading (independent of cell shape) for each cell it detects (Olson and Gittami, 2012). The smallest cell that the cell counter can detect is 4 um in effective diameter (assuming the cell is spherical). The *Scenedesmus dimorphus* cells could grow individually or grow together in clusters, arranging side by side up to 3 to 6 cells. The cell counter is not able to distinguish individually grown cells from cells grown in clusters.

Figure 4.8 shows the cell count measurements on day 4 and 8 from Experiment 2, Block 3 and 4. It is evident that the cell size distribution in the measurable range is not of a Gaussian distribution. Since many algae cells might be smaller than 4 um, the cell counter might have failed to detect a significant portion of the algae cells in the samples. The fact that the MOXI cell counter detected significant numbers of particles with effective greater that 5 um indicates that these cells were likely in clusters.

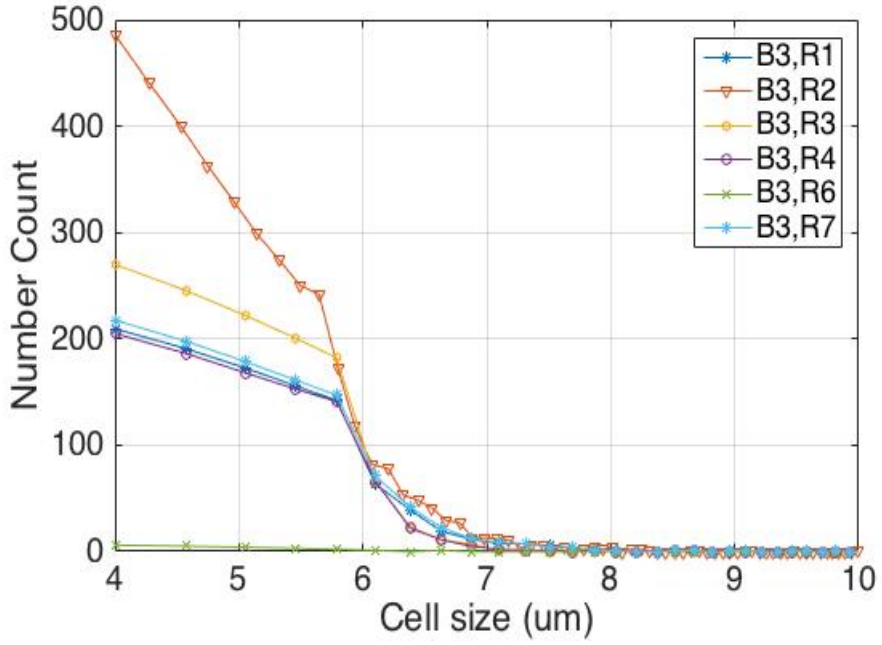

a) Exp 2, Block 3, in day 4

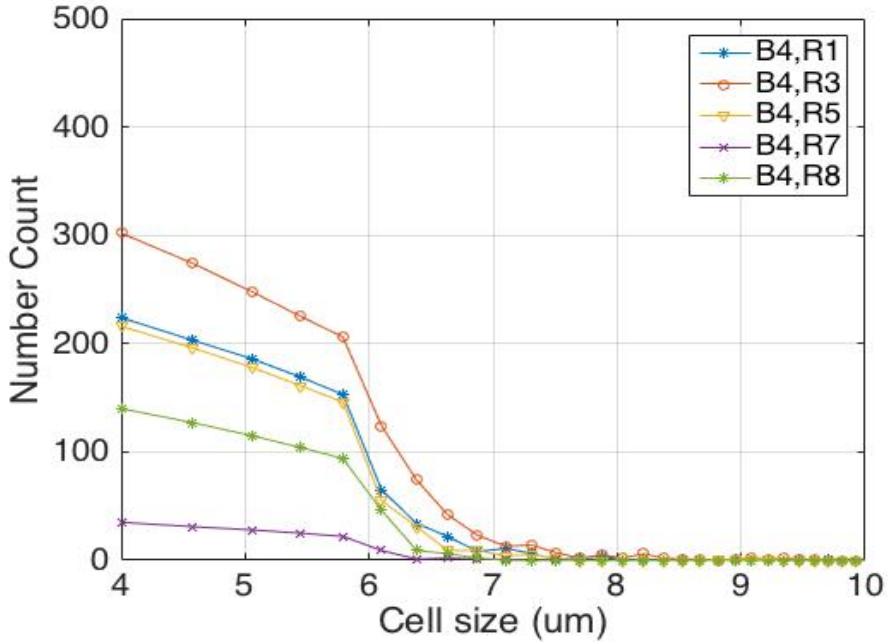

b) Exp 2, Block 4, in day 4

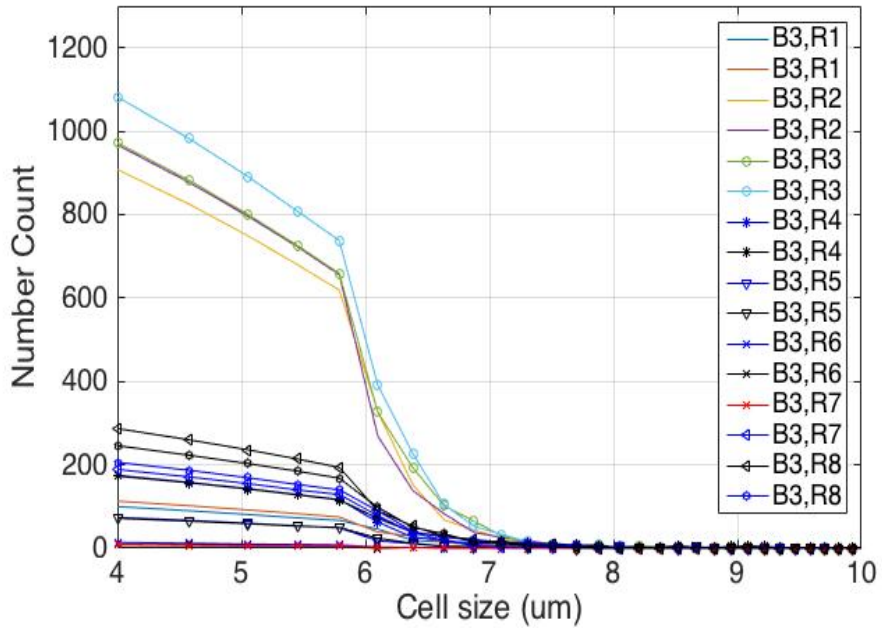

c) Exp 2, Block 3, in day 8

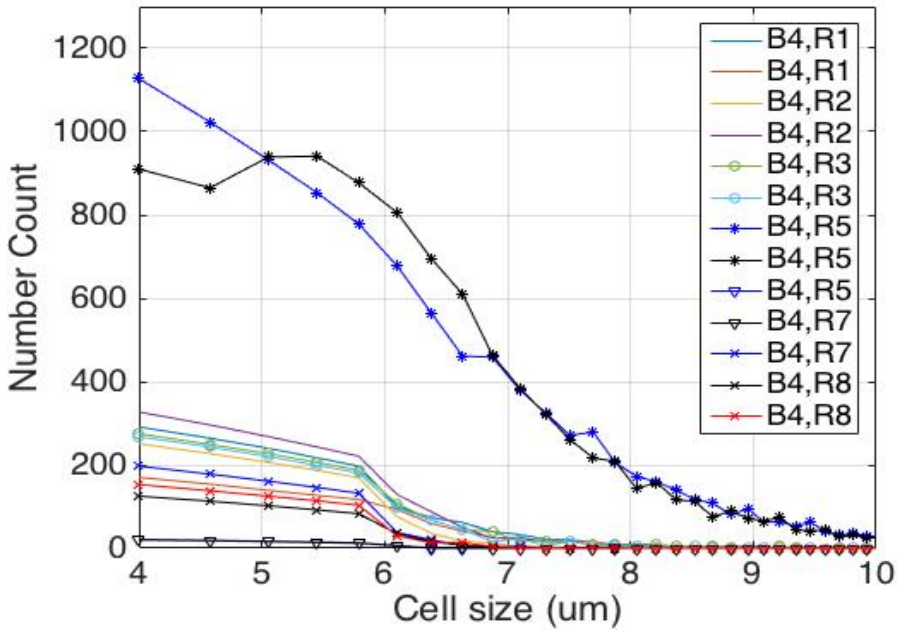

d) Exp 2, Block 4, in day 8

Figure 4.8: Experiment 2 Block 3 and 4 cell size distributions on day 4 and 8.

The total algae cells numbers that the cell counter detected altered with the $MgSO_4$ and the *K-P* concentrations in the growth media. Figure 4.9 a shows the effects of $MgSO_4$ and *K-P* on total cell number counts that were measured on day 4. The absorbance values for the runs were about 0.30 to 0.38 on that day, and the algae cells were in the exponential growth phase. The result indicated adding either $MgSO_4$ or *K-P* would increase number of large algae cells (cell diameter > 4 um). The run with no $MgSO_4$ nor *K-P* added (Block 3, Run 6) had an absorbance value of 0.37 on day 4, but only had a total of 22 cells detected by the cell counter. The center point (Block 3, run 3) had about the same absorbance (0.34) and had several thousands of large algae cells. It is expected that absorbance value depends on both cell number and cell size. The results seem to indicate that the additions of $MgSO_4$ and *K-P* result in the algae cells increasing in size and/or being in clusters, while no or low $MgSO_4$ and *K-P* would lead to greater number of smaller and individual cells.

At Day 8, most runs were either getting close to or at the stationary phase. Absorbance readings ranged from 0.45 to 0.85. Figure 4.9 b shows total numbers of large algae cells were strongly dependent on $MgSO_4$ concentration and less dependent on *K-P*.

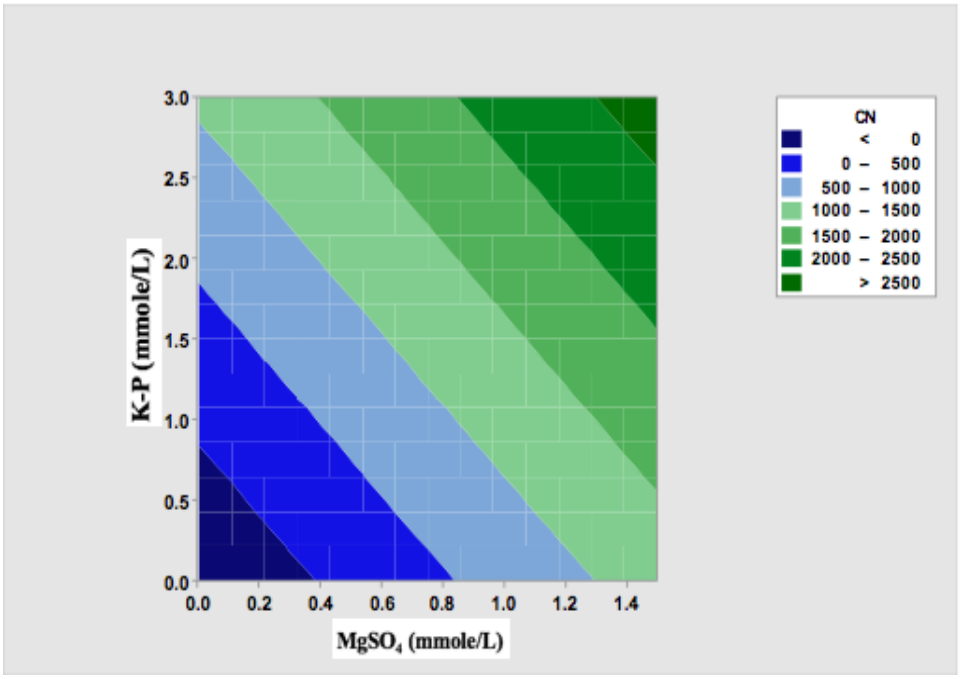

a) Exp 2, block 3 and 4 in day 4

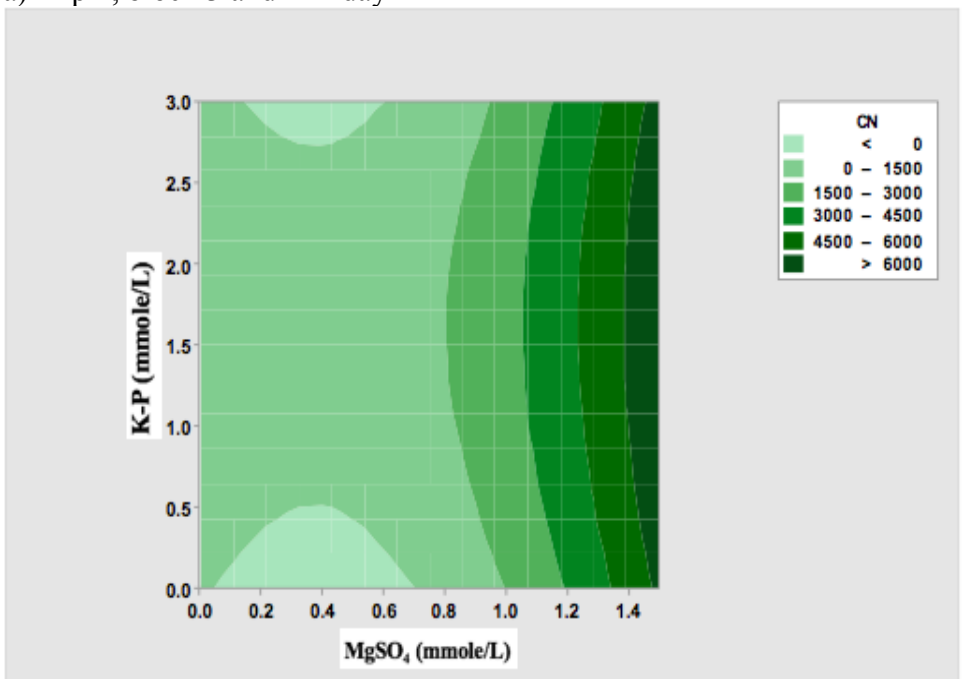

b) Exp 2, block 3 and 4 in day 8

Figure 4.9: Contour plot of total numbers of large algae cells ($D > 4$ um) vs. $MgSO_4$ and *K-P* for Experiment 2, Block 3 and 4, taken on a) day 4 and b) day 8.

4.6 Effects of Digestate on u_g, X_{max}, r, P_a, and P_i

The effect of digestate on process parameters was only examined in Experiment 1. Algae growth may be affected by two features of the digestate: nutrient levels and light permeability. Digestate contains nutrients for grow algae, and thus digestate dilution would lead to decrease in nutrient levels. According to Michaelis-Menten kinetics, when nutrient concentrations are below the saturated level, the algae grow rate decreases. On the other hand, high nutrient levels might inhibit algae growth. Nevertheless, all major elemental nutrients in 2% digestate (ICP-MS data) are lower than those in the 3N-BB media. Nutrient levels of the maximum digestate concentration media (up 1.817% digestate (v/v)) should not cause algae growth inhibition.

Another factor is the digestate turbidity. The growth media turbidity increases as digestate concentration increases. Increase turbidity might cause a decrease in light permeation through the growth media, which would decrease the algae growth rate. As shown on Figure 4.10, the Experiment 1 regression model predicts that the maximum growth rate would increase as digestate concentration increases until reaches 1.0 v/v% dilution. Further increases in digestate level would result decrease in the maximum growth rate. This descrease might be caused by the increase in turbidity as the digestate levels increase in the growth media.

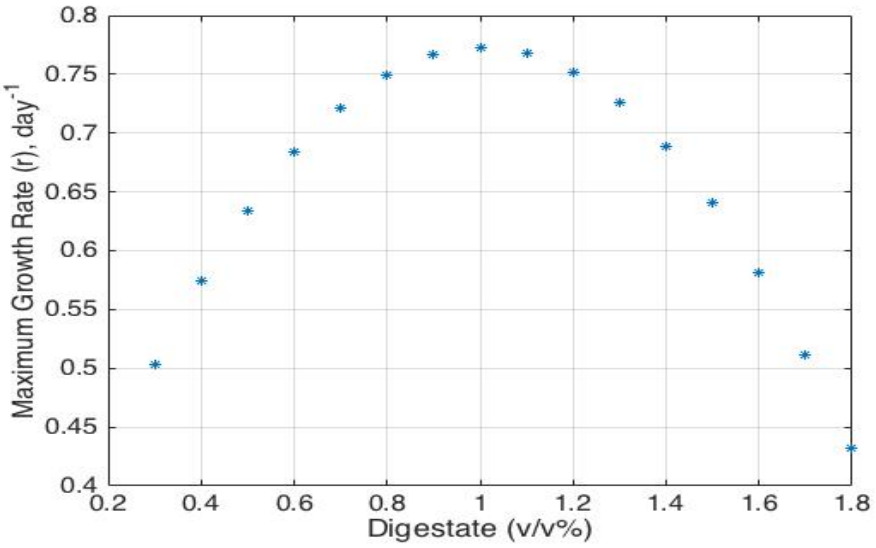

Figure 4.10: Effect of digestate on maximum growth rate with $MgSO_4$=0.61 mmole/L and P=2.81 mmole/L (estimated with the *r* regression equation in Table VII for Exp. 1).

The response surface regression model equation for X_{max} as a function of digestate concentration is shown in Figure 4.11. Maximum algae concentration shows here in unit of A_{600} absorbance readings, and these readings are linearly proportional to algae concentration. In theory, maximum algae concentration should increase with amount of growth media nutrients contents until the maximum algae concentration reaches the maximum growth capacity of the batch reactor. According to our results, the maximum growth capacity of the reactor is may be achieved at digestate concentration above 1.8% (v/v), indicating that the digestate turbidity at 1.8% was not high enough to limit total biomass assimilation.

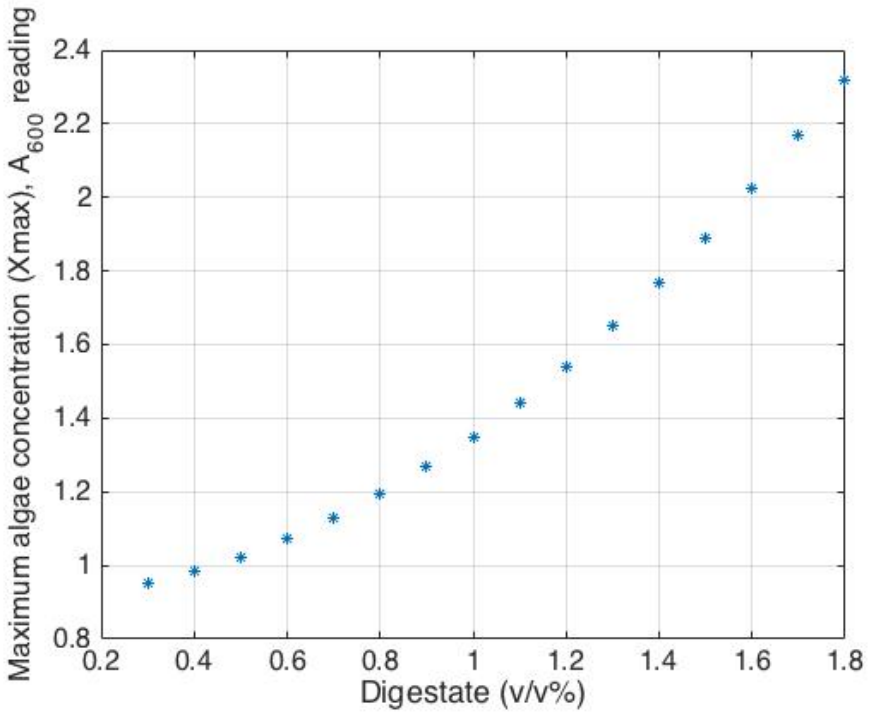

Figure 4.11: Effect of digestate on maximum algae concentration with $MgSO_4$=0.61 mmole/L and P=2.81 mmole/L (estimated with the *Xmax* regression equation in Table VII for Exp. 1).

Figure 4.12 and Figure 4.13 show the average biomass productivity (P_{a90}) and the maximum instantaneous biomass productivity ($P_{i\max}$) as a function of percentage digestate dilution. The Experiment 1 models show that the highest average biomass productivity (between 1.9 to 2.0 day^{-1}) and the highest maximum instantaneous biomass productivity (0.28 day^{-1}) are obtained at around 1.4% digestate. Specific growth rate (u_g) increases continuoursly with digestae, up to the tested valaue of 1.8% (Figure 4.14). The rate of increase in the specific growth rate slows down and becomes steady as digestate concentration approaches 1.5% v/v.

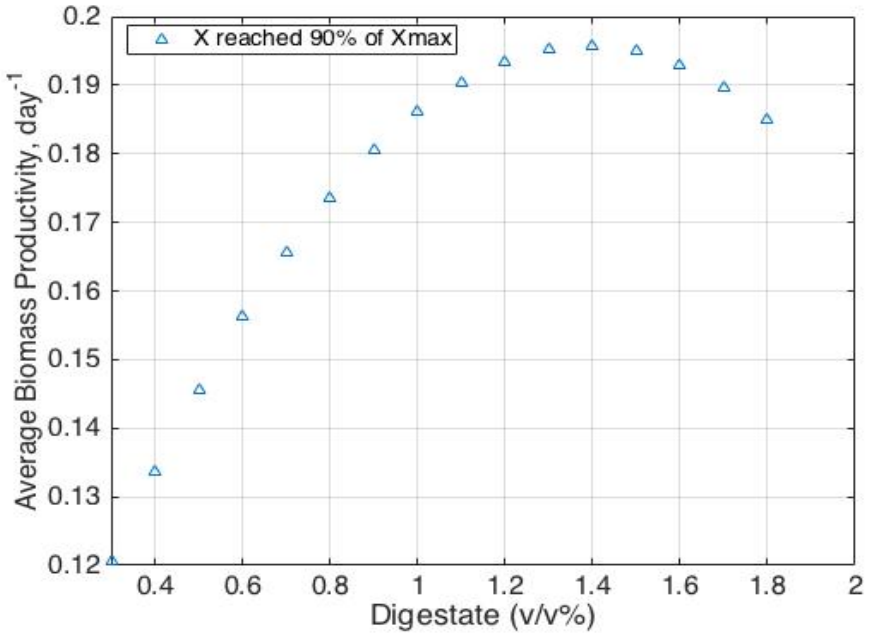

Figure 4.12: Effect of digestate on average biomass productivity with $MgSO_4$=0.61 mmole/L and P=2.81 mmole/L (estimated with the P_{a90} regression equation in Table VII for Exp. 1).

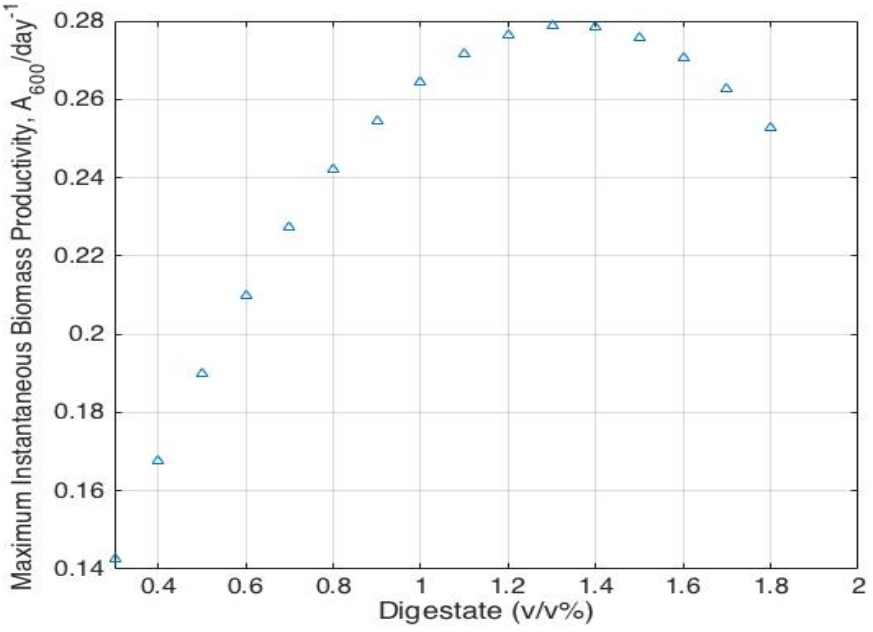

Figure 4.13: Effect of digestate on maximum instantaneous biomass productivity with $MgSO_4$=0.61 mmole/L and P=2.81 mmole/L (estimated with the $P_{i\max}$ regression equation in Table VII for Exp. 1).

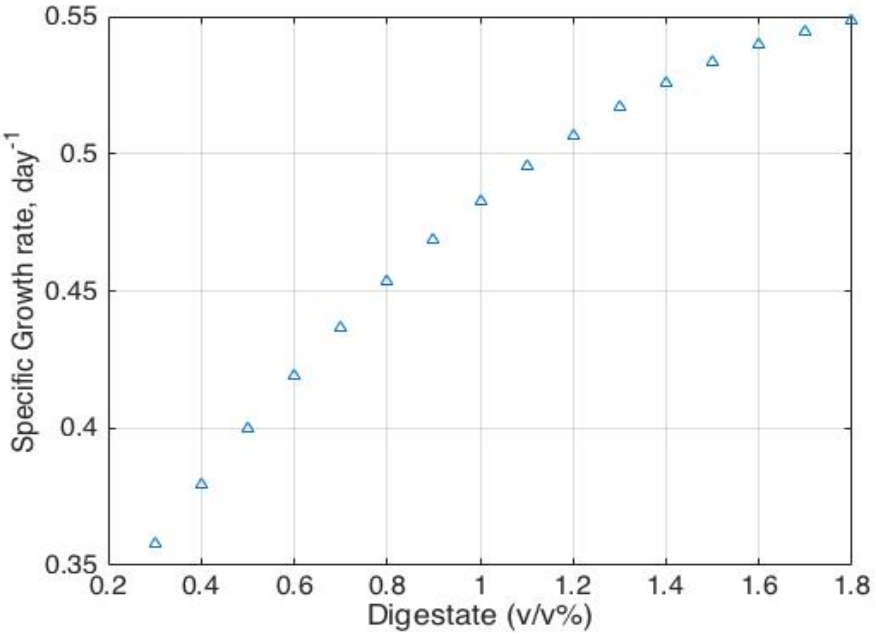

Figure 4.14: Effect of digestate on specific growth rate with $MgSO_4$=0.61 mmole/L and P=2.81 mmole/L (estimated with the u_g regression equation in Table VII for Exp. 1).

4.7 Effects of $MgSO_4$ and K-P on u_g, X_{max}, r, P_a, and P_i

According to the surface regression models that developed based on these two sets of experiments, the effects of $MgSO_4$ and K-P appear to be independent of the digestate, but they are dependent on each other. Contours plots in Figure 4.15 showed the effect of $MgSO_4$ and K-P on maximum growth rate and Figure 4.16 on maximum algae concentration. At concentrations lower than those of the Experiment 1 center point ($MgSO_4$ = 0.61 mmol/L and K-P = 2.81 mmol/L), both Experiment 1 and Experiment 2 showed that by decreasing the $MgSO_4$ and K-P levels, higher maximum growth rate (r) was obtained, but low maximum algae concentration (X_{max}) was yielded. The r and X_{max} were found by using the daily absorbance data. Both algae cell number and cell size in growth media affect the absorbance reading at A_{600}. These results might be caused by a faster cell division rate and smaller cell size growth as the K-P and $MgSO_4$ concentrations decrease. Experiment 2 cell size and number measurements showed that the algae growth under no K-P and $MgSO_4$ condition only resulted less than 30 large algae cells (cell diameter > 4 um), while at Experiment 2 center point ($MgSO_4$ = 0.75 mmol/L and K-P = 1.5mmol/L), the absorbance reading was similar (at the time of measurement), but more than thousand cells were detected. This indicates that the algae cell size might get smaller but the number of cells would get higher as the K-P and $MgSO_4$ concentrations decrease.

Regression equation for Experiment 1 also showed the K-P and $MgSO_4$ concentrations increase beyond the $MgSO_4$ of 0.8 mmol/L and K-P of 3.8 mmol/L concentrations would yield higher maximum growth rate (r) but the maximum algae concentration (X_{max}) is lower. The cause to these results is unknown. At these high K-P and $MgSO_4$ concentrations, the algae cells might grow in a similar way as to those of no K-P and

$MgSO_4$ addition. Since it would be adding costs to grow algae at high $MgSO_4$ and *K-P* concentrations, and the resulting maximum growth rate might not be better than those of growing algae at no $MgSO_4$ and *K-P* addition. Experiment 2 did not try to examine the algae growth at these high $MgSO_4$ and *K-P* concentrations.

The contour plots for *Xmax* (Figure 4.16) show contradictions between Experiments 1 and 2. Experiment 1 predicts the *Xmax* would increase as the *K-P* concentration decreases while increase the $MgSO_4$ concentration in low right corner region of the Experiment 1 contour plot ($MgSO_4$ > 0.6 mmol/L and *K-P* < 3 mmol/L). However, Experiment 2 predicts the *Xmax* would increase as *K-P* and $MgSO_4$ concentrations increase in this concentration region. The contradictions might be due to the limitation on the surface response regression equation. The highest hierarchal term in the regression equation is quadratic. Experiment 1 tested wide range of *K-P* concentration (0.0 to 5.6 mmole/L), the shape of the curves might not be able to describe the region well. Experiment 2 tested narrower range of *K-P* concentration (0.0 to 3.0 mmole/L), from which the results might be more accurate.

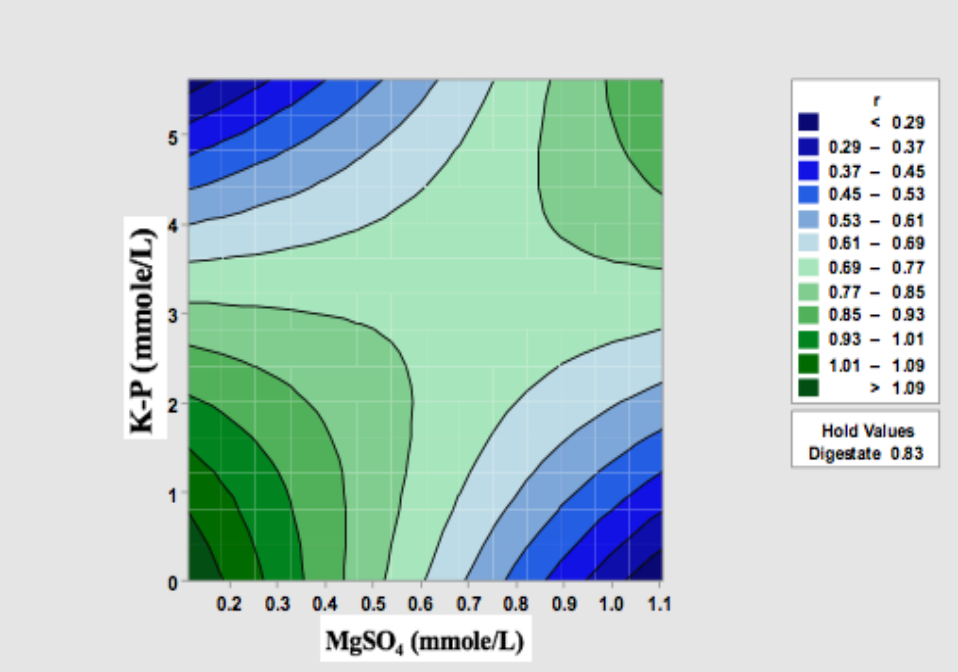

a) Contour plot of maximum growth rate vs. *MgSO₄* and *K-P* for Experiment 1

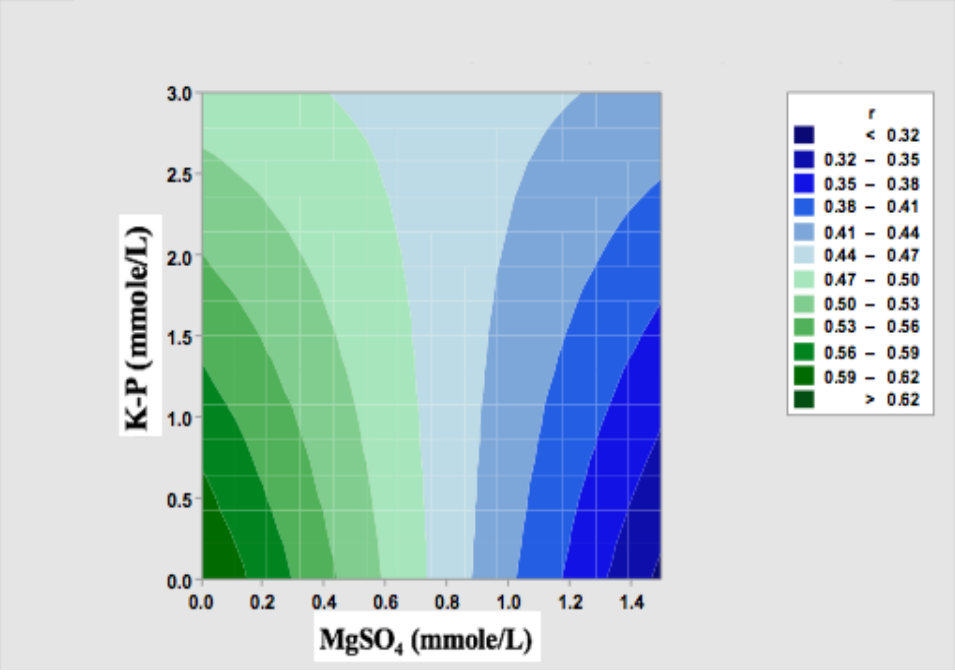

b) Contour plot of maximum growth rate vs. *MgSO₄* and *K-P* for Experiment 2

Figure 4.15: Effects of *MgSO₄* and *K-P* on maximum growth rate a) Experiment 1, b) Experiment 2 (estimated with the *r* regression equation on Table VII and VIII).

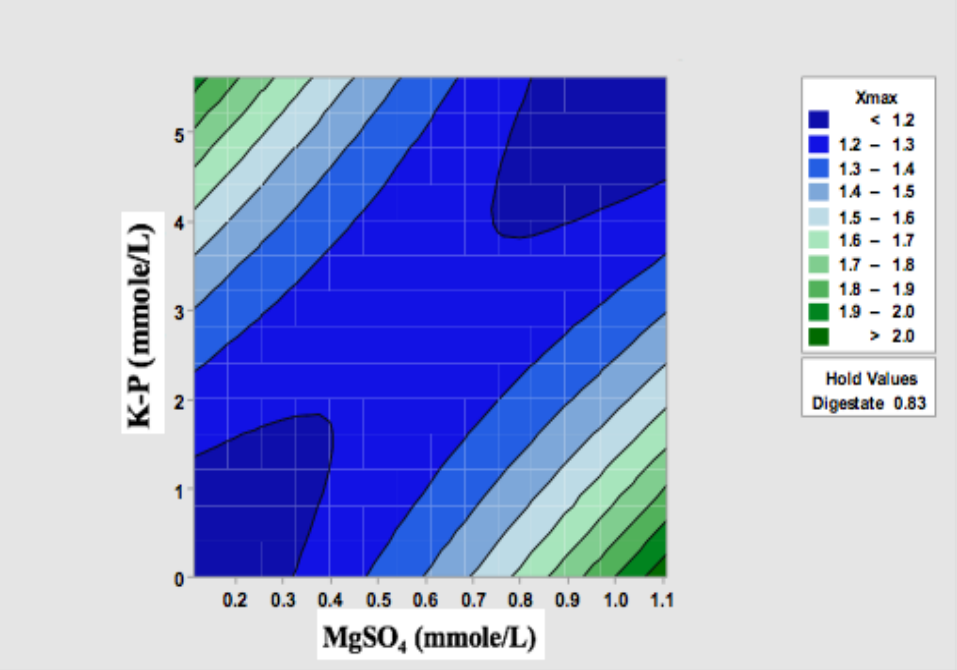

a) Contour plot of Xmax vs. *K-P*, *MgSO₄* for Experiment 1

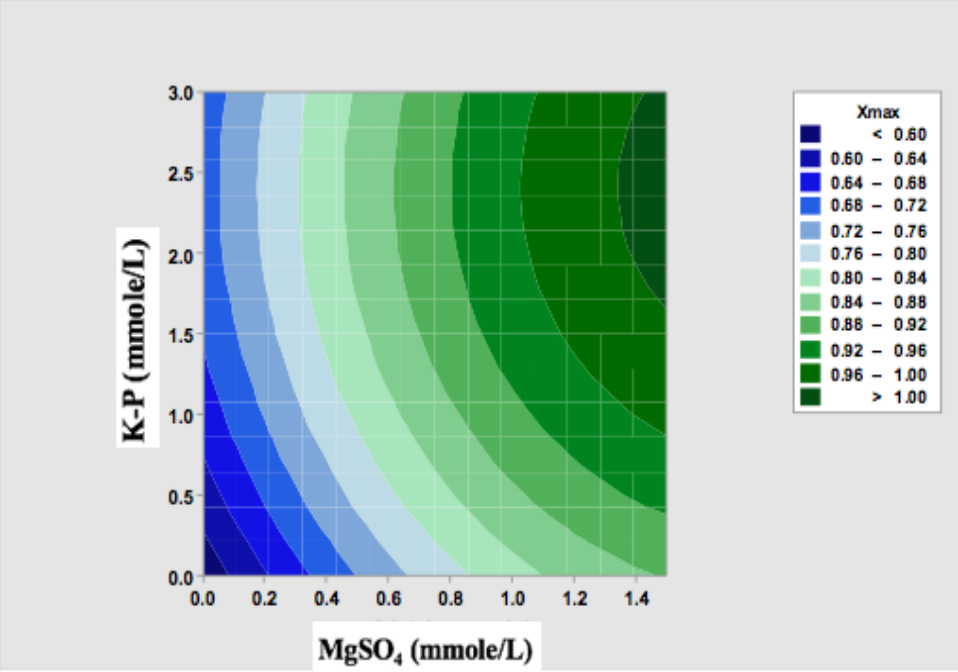

b) Contour plot of *Xmax* vs. *K-P*, *MgSO₄* for Experiment 2

Figure 4.16: Effect of *MgSO₄* and *K-P* on maximum growth rate a) Experiment 1, b) Experiment 2 (estimated with the X_{max} regression equation on Table VII and VIII).

Surface response regression equations were generated with Experiment 1 data for average biomass productivity as X reaching 90% of X_{max} (P_{a90}) and maximum instantaneous biomass productivity ($P_{i\max}$). As shown in Figure 4.17 and Figure 4.18, the Experiment 1 P_{a90} regression model and $P_{i\max}$ regression model suggest the amounts of *K-P* and $MgSO_4$ should be both at either lower or higher concentrations than the center point at the same time. For Experiment 2, the linear regression method was not able to generate a model for P_{a90} and $P_{i\max}$. The ranges of *K-P* and $MgSO_4$ concentrations that were tested did not show significant effects on P_{a90} and $P_{i\max}$.

Specific growth rate (u_g) regression equation had high goodness of fit for Experiment 1 ($r^2 = 97.28\%$). The regression model showed adding *K-P* would decrease the specific growth rate. There was also an interaction term between digestate and *K-P*, which suggested both digestate and *K-P* should be kept at high or low levels at the same time. The r-square value for Experiment 2 u_g regression model was 88.64%, and the model indicated adding either *K-P* or $MgSO_4$ would decrease the specific growth rate.

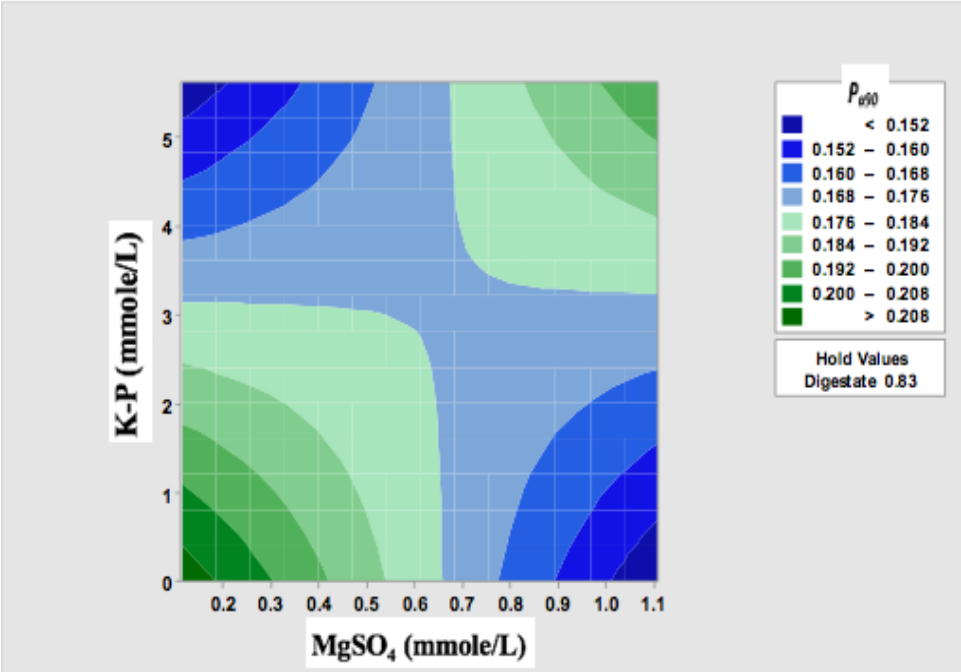

Figure 4.17: Effect of *MgSO₄* and *K-P* on Experiment 1 P_{a90} (estimated with the P_{a90} regression equation on Table VII)

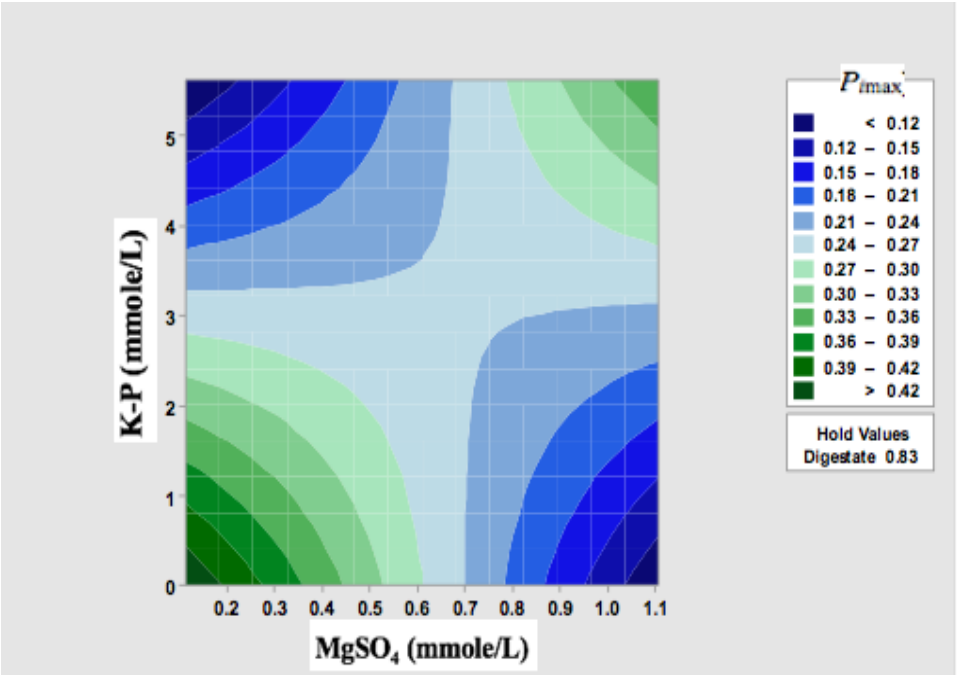

Figure 4.18: Effect of *MgSO₄* and *K-P* on maximum instantaneous biomass productivity for Experiment 1 (estimated with the P_{imax} regression equation on Table VII).

4.8 Experimental Errors

Differences are seen in between these two experimental results as presented above. Possible experimental errors are discussed in this section. First, the total sampling volume is greater than 10% of the batch reactor working volume, which is about 14% to 17%. The vaporization rate might not hold constant over time. The absorbance volume measurements near the end of the batch reactor run might be higher than the actual values.

Four center point runs are compared in Figure 4.19. Center point 1 is from the Experiment 1 data, while other three center points were collected after Experiment 1 was completed. The digestate, $MgSO_4$, *K-P* concentrations of these four center point runs are listed in Table IX, and the resulting four parameters of the non-linear logistic equations are listed in Table X.

Table IX: Digestate, $MgSO_4$, *K-P* concentration in the center point runs.

	Digestate (v/v)	$MgSO_4$ **(mmole/L)**	*K-P* **(mmole/L)**
center point 1 (C1)	1.0%	0.61	2.81
center point 2 (C2)	1.0%	0.61	2.81
center point 3 (C3)	1.0%	0.563	2.788
center point 4 (C4)	1.0%	0.563	2.788

Table X: X_{min}, X_{max}, r, t_{50} for the four center points.

	C1	**C2**	**C3**	**C4**
X_{min}	0.02	-0.03	0.02	-0.05
X_{max}	1.42	1.02	1.49	1.30
r	0.74	0.55	0.56	0.48
t_{50}	4.03	4.07	5.56	4.72

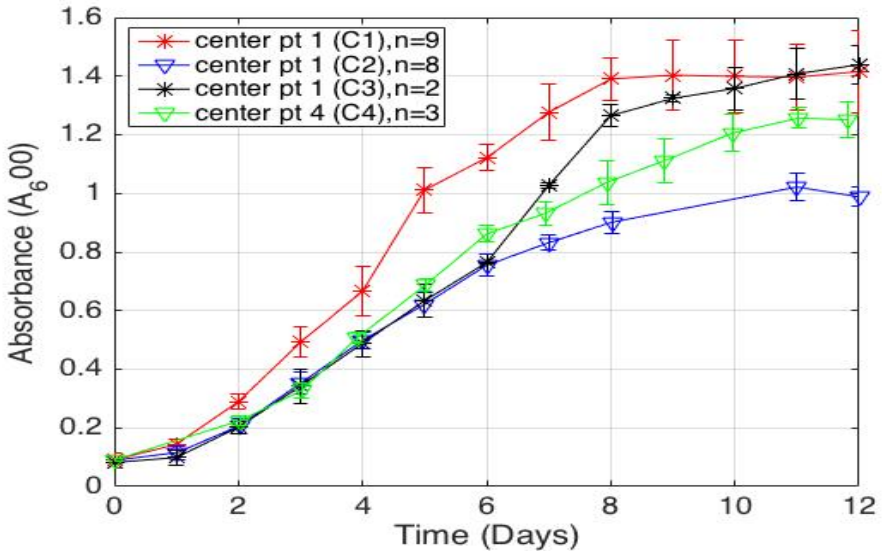

Figure 4.19: Absorbance at A600 vs. time for the four center points.

Comparing the maximum growth rate, center point 1 ($r = 0.74\ day^{-1}$) is significantly higher than the remaining three center points, ranging from 0.48 to 0.56 day^{-1}, and the average biomass productivity and instantaneous biomass productivity are also about 30% higher than those of the remaining. These differences may be attributable to absorbance measurement errors and algae cell source differences.

The same alga specie was used for all four center points. Nevertheless, the algae inoculum source for Center point 1 was from a different algae inoculum bottle than other three center points. Some unknown ingredients in the first algae inoculum bottle may have made these algae cells grow faster, which could have caused different growth curve for center point 1 as shown in Figure 4.19.

Another cause of the discrepancy may stem from to the method of absorbance measurements. Absorbance value (A_{600}) is not linearly related to algae cell concentration beyond absorbance values of 1.0. The samples with values above 0.9 were diluted with D.I. water and measured again. Dilution might have caused errors in the absorbance

reading. As shown on Figure 4.19, the rates of change in absorbance were approximately the same up to Day 6 for center points 3 and 4. The differences in the rates of change in absorbance happened at Day 7, when the absorbance reading went above 0.9 for both center points, and dilution took place. In addition, the rates of change in absorbance in center point 3 run is the greatest in between Day 6 to Day 8, which is after t_{50}, which is about 5.56 days. According to the four parameter logistic model, the rate of change in absorbance should decrease after t_{50}.

Using nonlinear regression contains inherent risk, for which the linearity would only keep within certain range of the data. The four-parameters logistic equation (Equation 2.4) could rewrite in a linear form as follow:

Equation 4.5:

$$\ln\left(\frac{X_{max} - X_{min}}{X - X_{min}} - 1\right) = -r(t - t_{50})$$

The equation is plotted in Figure 4.20 with *r* as the slope for a batch reactor run in Experiment 2 (Block 3, Run 2). The results indicate the linearity of this equation hold true for most data points, and small deviations are seen at the beginning and ending of the batch reactor run.

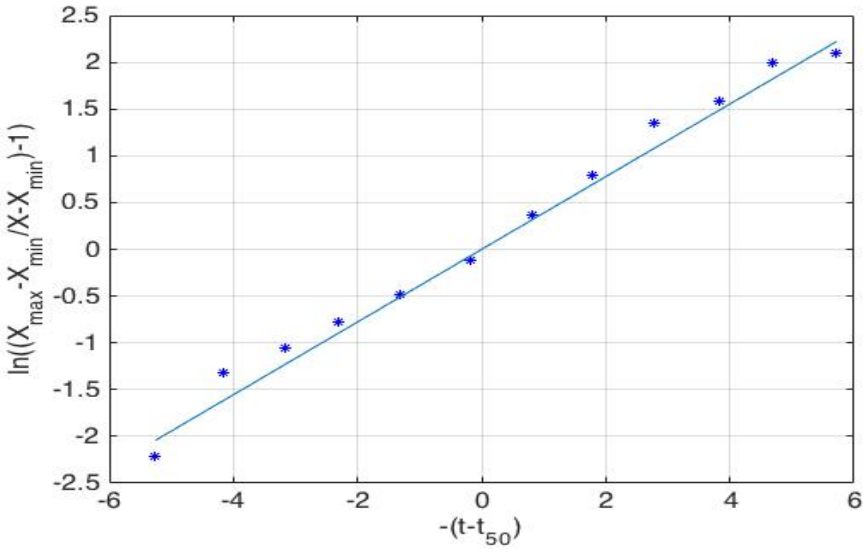

Figure 4.20: linearity checks on logistic model equation with *r* as the slope for a batch reactor run in Experiment 2 (Block 3, Run 2).

CHAPTER V

CONCLUSIONS AND RECOMMENDATIONS

5.1 Conclusions

Two experimental sets were gathered to study the effects of digestate, *K-P* and $MgSO_4$ on algae growth. The results suggested that digestate was the most essential factor among these three factors. Moderate concentrations of digestate (1%) yield high maximum growth rate, while high digestate concentrations (>1.0%) limit the maximum growth rate by limiting the light penetration through the growth media, but yield high maximum algae concentration in batch growth mode. Nevertheless, this experiment did not identify the digestate concentration that would provide enough nutrients for the algae concentration to reach the maximum growth capacity in a batch reactor, or when the light penetration becomes limited. To maximize biomass production efficiency, digestate should be kept at 1.4% (v/v) dilution, which would give highest average biomass productivity and instantaneous biomass productivity. There might be more timely feasible to stop the batch experiments when the algae concentration reaches 90% of X_{max} where the average biomass productivity starts to decrease sharply. To run in CSTR reactor mode, the algae concentration should be maintained at 50% of the maximum

algae concentration, while manipulating the nutrients levels to maximize the instantaneous biomass productivity.

The digestate effect is mostly independent of both *K-P* and $MgSO_4$. A change in digestate concentrations would not be expected to influence the effects of *K-P* and $MgSO_4$ on algae growth. However, an interaction term was found between *K-P* and $MgSO_4$. When the concentrations of these two factors are lower than those of the Experiment 1 center point, both experiments 1 and 2 showed that decreases the *K-P* and $MgSO_4$ concentrations would yield higher maximum growth rate. However, in trade off, the maximum algae concentration might be lower. The cause might be the algae cells undergo faster cell division at lower *K-P* and $MgSO_4$ concentrations, while increase the concentrations may cause cells to increase in size and/or stay attached, and yield higher maximum algae concentrations at the end of the batch growth.

Experiment 1 results suggest high $MgSO_4$ (>0.8 mmol/L) and *K-P* (>3.8 mmol/L) concentrations also give high maximum growth rate (*r*) but lower maximum algae concentration (X_{max}). This interaction effect was not observed at lower *K-P* concentration (>3.8 mmol/L) even when the $MgSO_4$ level got higher (>1.5 mmol/L) as tested in Experiment 2. Since it would be adding costs to grow algae at these high $MgSO_4$ and *K-P* concentrations, and the resulting maximum growth rate might not be higher than those of growing algae at no $MgSO_4$ and *K-P* addition. The $MgSO_4$ and *K-P* addition to the diluted digestate growth media should be kept at minimum.

The specific growth rate is growth parameters to characterize the algae growth but it only captures the growth rate during the exponential growth phase, and fewer data points were used in the estimation. This method also involves visual inspection to determine the

data points that were used in the growth rate estimation and could introduce more subjective errors than the four-parameters logistic model. Both Experiments 1 and 2 suggest that an increased digestate concentration would increase the specific growth rate. On another hand, increasing the *K-P* and $MgSO_4$ concentrations would decrease the specific growth rate.

Differences in the growth parameters were observed between Experiments 1 and 2, in which Experiment 1 results were higher than those of Experiment 2. In comparing the four center points, absorbance measurement errors and algae cell source differences might be the cause to explain the difference.

5.2 Future Work

Recommendations to continue and expand this work are:

1. Daily measure and compare algae cell size distributions and concentration in growth media with or without *K-P* and $MgSO_4$ additions for a period of 12 days.
2. Grow algae at higher digestate concentrations, digestate dilution greater than 2% (v/v), to identify digestate concentrations that would limit the maximum algae concentration.
3. Combine the lipid and growth data from these two experiments to identify the optimum digestate, *K-P*, and $MgSO_4$ concentrations that would give the best lipid productivity.

Reference:

Abou-Shannab, R., Matter, I., Kim, S.-N., Oh, Y.-K., Choi, J., and Jeon, B.-H. (2011). Characterization and identification of lipid-producing microalgae species isolated from a freshwater lake. *Biomass and Bioenergy* (35), 3079-3085.

Anjos, M., Fernandes, B., Vicente, A., Teixeira, J., and Dragone, G. (2013). Optimization of CO_2 bio-mitigation by *Chlorella vulgaris*. *Bioresource Technology*, 149-154.

Bchir, F. S., Gannoun, H., Herry, S. E., and Hamdi, M. (2011). Optimization of *Spongiochloris sp.* biomass production in the abattoir digestate. *Bioresource Technology* (102), 3869-3876.

Bjornsson, W. J., Nicol, R. W., Dickinson, K. E., and McGinn, P. J. (2013). Anaerobic digestates are useful nutrient sources for microalgae cultivation: functional coupling of energy and biomass production. *J Appl Phycol* (25), 1523-1528.

Bollivar, *D*. (1997). Genetic analysis of chlorophyll biosynthesis. *Scholarship* (15).

Chalifour, A. and Juneau, P. (2011). Temperature-dependent sensitivity of growth and photosynthesis of *Scenedesmus obliquus*, *Navicula pelliculosa* and two strains of Microcystis aeruginosa to the herbicide atrazine. *Aquatic Toxicoloty* (103), 9-17.

Chen, M., Li, J., Dai, X., and Sun, Y. (2011). Effect of phosphorus and temperature on chlorophyll a contents and cell sizes of Scenedesmus obliquus and Microcystis aeruginosa. *Limnology* (12), 187-192.

Fanesi, A., Raven, J., and Giordano, M. (2014). Growth rate affects the responses of the green alga *Tetraselmis suecica* to external perturbations. *Plant, Cell and Environment* (37), 512-519.

Franchino, M., Comino, E., Bona, F., and Riggio, V. A. (2013). Growth of three microalgae strains and nutrient removal from an agro-zootechnical digestate. *Chemosphere* (92), 738-744.

Gorman, C. (2014, 11 11). *Algenol*. Retrieved 02 02, 2016, from http://www.algenol.com/media/press-releases

Gouveia, L., and Oliveira, A. (2009). Microalgae as a raw material for biofuels production. *J Ind Microbiol Biotechnol* (36), 269-274.

Gu, N., Lin, Q., Li, G., Qin, G., Qin, G., Lin, J., and Huang, L. (2012). Effect of salinity change on biomass and biochemical composition of *nannochloropsis oculata*. *Journal of the World Aquaculture Society* (43).

Held, P. and Banks, P. (2012). Screening for optimal algal cell growth and neutral lipid production conditions in microplates. *Enzo Life Sciences*.

Ho, S.-H., Chen, C.-Y., Yeh, K.-L., Chen, W.-M., Lin, C.-Y., and Chang, J.-s. (2010). Characterization of photosynthetic carbon dioxide fixation ability of indigenous *Scenedesmus obliquus* isolates. *Biochemical Engineering Journal* (53), 57-62.

Hu, J., Yu, F., and Lu, Y. (2012). Application of Fischer-Tropsch synthesis in Biomass to Liquid conversion. *Catalysts , 2*.

Hulen, A. (2014, June 9). *Renewable Energy Group Completes Dynamic Fuels Acquisition*. Retrieved 02 01, 2016, from Renewable Energy Group: http://www.regfuel.com/news/2014/06/09/renewable-energy-group-completes-dynamic-fuels-acquisition

Ji, M.-K., Abou-Shanab, R., Hwang, J.-H., Timmes, T., Kim, H.-C., Oh, Y.-K., and Jeon, b. (2013). Removal of nitrogen and phosphorus from piggery wastewater effluent using the green microalga *Scenedesmus obliquus*. *Journal of Environmental*, 1198-1205.

Lemesle, V. and Mailleret, L. (2008). A mechanistic investigation of the algae growth ‘‘Droop’’ Model. *Acta Biotheor* (56), 87-102.

Li, X., Hu, H.-y., Gan, K., and Sun, Y.-x. (2010). Effects of different nitrogen and phosphorus concentrations on the growth, nutrient uptake, and lipid accumulation of a freshwater microalga *Scenedesmus sp*. *Bioresource Technology* (101), 5994-5500.

Mailleret, L., Gouze, J.-L., and Bernard, O. (2005). Nonlinear control for algae growth models in the chemostat. *Bioprocess Biosyst Eng* (27), 319-327.

Mandal, S. and Mallick, N. (2009). Microalga *Scenedesmus obliquus* as a potential source for biodiesel production. *Appl Microbiol Biotechnol* (84), 281-291.

Mandal, S. and Mallick, N. (2001). Waste utilization and biodiesel production by the green microalga *Scenedesmus obliquus. Applied and Environmental Microbiology* (77), 374-377.

Mandal, S. and Mallick, N. (2011). Waste utilization and biodiesel production by the green microalga *Scenedesmus obliquus. Applied and Environmental Microbiology* (77), 374-377.

Myers, J., Curtis, B. and Curtis W. (2013). Improving accuracy of cell and chromophore concentration measurements using optical density. *BioMed Central* (6:4).

RFA. (2015). *2015 Ethanol Industry Outlook.* Renewable Fuels Association.

Rodrigue, J.-P. and Comtois, C. (2013). *The geography of Transport systems* (3rd ed.). New York: Routledge.

Schwenk, J. (2010). Effects of magnesium sulfate, digestate, and other inorganic nutrients on the phototrophic growth of the green microalga, *Scenedesmus dimorphus.* Cleveland: Cleveland State Univeristy.

Sheehan, J., Dunahay, T., Benemann, J., and Roessler, P. (1998). *A Look Back at the U.S. Department of Energy's Aquatic Species Program—Biodiesel from Algae.* National Renewable Energy Laboratory.

Trelease, S. and Selsam, M. (1939). Influence of calcium and magnesium on the growth of *Chlorella, American Journal of Botany* (*26*), 339-341.

U.S. EIA. (2015). *Short-Term Energy Outlook December 2015.* U.S. Energy Information Administration.

Uggetti, E., Sialve, B., Latrille, E., and Steyer, j.-P. (2014). Anaerobic digestate as substrate for microalgae culture: the role of ammonium concentration on the microalgae productivity. *Bioresource Technology* (152), 437-443.

Welter, C., Schwenk, J., Kanani, B., Van Blargan, J., and Belovich, J. M. (2013). Minimal media for optimal growth and lipid production of the microalgae Scenedesmus dimorphus. *Enviromental Progress & Sustainable Energy* (32), 937.

Wijffels, R. and Barbosa, M. (2010). An outlook micro algal biofuels. *Science* (329), 796-799.

Wu, Y.-H., Yu, Y., Hu, H.-y., and Su, Z.-F. (2012). Biomass production of a *Scenedesmus sp.* under phosphorous-starvation cultivation condition. *Bioresource Technology* (112), 193-198.

Xu, X., Shen, Y., and Chen, J. (2015). Cultivation of *Scenedesmus dimorphus* for C/N/P removal and lipid production. *Electronic Journal of Biotechnology* (18), 46-50.

Xu, Y. and Boeing, W. (2014). Modeling maximum lipid productivity of microalgae: Review and next step . *Renewable and Sustainable Energy Reviews* (32), 29-39.

Yang, J., Rasa, E., Tantayotai, P., Scow, K., Yuan, H., and Hristova, K. (2011). Mathematical model of *Chlorella minutissima* UTEX2341 growth and lipid production under photoheterotrophic fermentation conditions. *Bioresource Technology* (102), 3077-3082.

Yoo, C., Jun, S.-Y., Lee, J.-Y., Ahn, C.-Y., and Oh, H.-M. (2009). Selection of microalgae for lipid production under high levels carbon dioxide. *Bioresource Technology* (101), S71-S74.

Zhang, Z., Sachs, J., and Marchetti, A. (2009). Hydrogen isotope fractionation in freshwater and marine algae: II. Temperature and nitrogen limited growth rate effects. *Organic Geochemistry* (40), 428-439.

APPENDIX A

Logistic Growth Model Integration

Variable	Definition	Unit
u	algae growth rate	$time^{-1}$
r	Maximum growth rate	$time^{-1}$
X	Population at a given time	(Absorbance value or concentration unit)
t	Time	Days
$\boldsymbol{X_{max}}$	*Maximum carrying population*	(Absorbance value or concentration unit)
$\boldsymbol{X_o}$	*Minimum carrying population*	(Absorbance value or concentration unit)
$\boldsymbol{t_{50}}$	Time when population reached half of the *Maximum carrying population*	Days

For a given growth condition, specific growth rate is not constant and depending on the maximum growth rate, population at the time, and maximum carrying population as shown in the following equation:

$$u = r\ (1 - \frac{X}{X_{max}}) \tag{1}$$

For a given growth condition, the rate of the population change is also depending on *maximum growth rate, population at the time, and maximum carrying population at a given growth condition as shown in the following equation:*

$$\frac{dX}{dt} = r\ X\ (1 - \frac{X}{X_{max}}) \tag{2}$$

To integrate Equation 2, variables are first separated,

$$\frac{dX}{X\ (1-\frac{X}{X_{max}})} = r\ dt \tag{3}$$

Partial fractions decomposition is applied to the left-hand-side of Equation 3,

$$\frac{dX}{X} + \frac{\frac{1}{X_{max}}dX}{(1-\frac{X}{X_{max}})} = r\ dt \tag{4}$$

Assuming at $t=t_{min,}$ $X=X_{min}$ but not zero, substitute $X-X_{min}$ for the original X, and $X_{max}-X_{min}$ for original X_{max},

$$\frac{dX}{X-X_{min}} + \frac{\frac{1}{X_{max}-X_{min}}\,dX}{(1-\frac{X-X_{min}}{X_{max}-X_{min}})} = r\,dt \tag{5}$$

Each term on Equation 5 are integrated,

$$\int \frac{dX}{X-X_{min}} = \ln(X-X_{min}) + C_1$$

$$\frac{1}{X_{max}-X_{min}} \int \frac{dX}{(1-\frac{X-X_{min}}{X_{max}-X_{min}})} = -\ln\left(1-\frac{X-X_{min}}{X_{max}-X_{min}}\right) + C_2$$

$$\int r\,dt = r\,t + C_3$$

By combining the above integrated terms,

$$[\ln(X-X_{min}) + C_1] + \left[-\ln\left(1-\frac{X-X_{min}}{X_{max}-X_{min}}\right) + C_2\right] = [r\,t + C_3] \tag{6}$$

Let $k = C_3 - C_1 - C_2$, and simplifies the Equation 6,

$$\ln\left[\frac{X-X_{min}}{1-\frac{X-X_{min}}{X_{max}-X_{min}}}\right] = rt + k \tag{7}$$

Let $C = e^k$,

$$\frac{X-X_{min}}{1-\frac{X-X_{min}}{X_{max}-X_{min}}} = e^{rt+k} = Ce^{rt} \quad \text{Or} \qquad X - X_{min} = \frac{Ce^{rt}}{1+\frac{Ce^{rt}}{X_{max}-X_{min}}} \tag{8}$$

By assuming at $t = t_{50}$, $X_{50} - X_{min} = \frac{X_{max}-X_{min}}{2}$, then

$$C = \frac{2(X_{50}-X_{min})}{e^{rt_{50}}} = \frac{(X_{max}-X_{min})}{e^{rt_{50}}} \tag{9}$$

With substituting the value of C in Equation 9 into Equation 8,

$$X = X_{min} + \frac{(X_{max}-X_{min})}{1+e^{-r\,(t-t_{50})}} \tag{10}$$

APPENDIX B

Table XI: Standard errors for Experiment 1 X_{min}, X_{max}, r, t_{50}, and u_g.

Block	**MgSO4 coded**	**K-P Coded**	***D* coded**	X_{min}	X_{max}	r	t_{50}	u_g
1	1	-1	1	0.290	0.269	0.085	0.503	0.162
1	0	0	0	0.087	0.041	0.095	0.250	0.149
1	0	0	0	0.108	0.052	0.133	0.313	0.142
1	0	0	0	0.073	0.034	0.084	0.202	0.172
1	-1	-1	-1	0.112	0.034	0.103	0.374	0.255
1	1	1	-1	0.099	0.039	0.090	0.323	0.133
1	0	0	0	0.065	0.033	0.106	0.189	0.142
1	-1	1	1	0.337	0.294	0.095	0.579	0.210
2	0	0	0	0.044	0.021	0.166	0.134	0.090
2	-1	1	-1	0.177	0.046	0.114	0.639	0.236
2	0	0	0	0.043	0.016	0.083	0.131	0.074
2	1	-1	-1	0.177	0.058	0.134	0.627	0.306
2	1	1	1	0.079	0.053	0.119	0.224	0.153
2	-1	-1	1	0.064	0.045	0.138	0.186	0.101
2	0	0	0	0.037	0.017	0.071	0.12	0.171
2	0	0	0	0.042	0.020	0.100	0.150	0.165
3	0	0	0	0.067	0.021	0.089	0.182	0.295
3	0	-1.633	0	0.075	0.025	0.095	0.208	0.274
3	0	1.633	0	0.070	0.021	0.098	0.193	0.172
3	0	0	-1.633	0.034	0.063	0.299	0.315	0.734
3	-1.633	0	0	0.037	0.015	0.076	0.108	0.154
3	0	0	1.633	0.072	0.048	0.456	0.04	0.205
3	1.633	0	0	0.058	0.021	0.075	0.171	0.195
3	0	0	0	0.05	0.02	0.07	0.141	0.128

Table XII: Standard errors for Experiment 2 X_{min}, X_{max}, r, t_{50}, and u_g.

BLOCK	$MgSO_4$ coded	K-P Coded	X_{min}	X_{max}	r	t_{50}	u_g
1	-1	1	0.028	0.019	0.066	0.192	0.094
1	-1	-1	0.024	0.009	0.089	0.157	0.032
1	1	0	0.029	0.300	0.063	0.197	0.020
1	1	-1	0.134	0.033	0.071	0.785	0.153
1	-1	1	0.100	0.028	0.087	0.587	0.131
1	-1	-1	0.055	0.021	0.160	0.385	0.158
1	1	0	0.100	0.065	0.097	0.447	0.079
1	1	-1	0.268	0.067	0.106	1.600	0.169
2	-1	-1	0.105	0.018	0.112	0.551	0.293
2	0	1	0.055	0.027	0.057	0.297	0.156
2	0	-1	0.076	0.018	0.072	0.475	0.186
2	1	1	0.035	0.063	0.052	0.247	0.022
2	-1	-1	0.041	0.11	0.039	0.236	0.157
2	0	1	0.066	0.040	0.079	0.340	0.103
2	0	-1	0.332	0.042	0.117	1.970	0.078
2	1	1	0.055	0.037	0.032	0.203	0.046
3	0	0	0.072	0.055	0.076	0.035	0.048
3	1	1	0.061	0.070	0.071	0.324	0.061
3	1	-1	0.045	0.046	0.071	0.264	0.023
3	-1	1	0.024	0.012	0.035	0.348	0.058
3	0	0	0.038	0.031	0.067	0.184	0.073
3	-1	-1	0.024	0.006	0.046	0.167	0.131
3	0	0	0.082	0.053	0.113	0.424	0.065
3	0	0	0.046	0.037	0.066	0.250	0.030
4	0	0	0.104	0.095	0.107	0.464	0.063
4	0	0	0.100	0.120	0.080	0.452	0.080
4	0	1	0.070	0.053	0.111	0.323	0.058
4	0	0	0.038	0.035	0.046	0.178	0.060
4	1	0	0.225	0.214	0.142	0.822	0.157
4	0	0	0.055	0.024	0.078	0.338	0.119
4	-1	0	0.143	0.051	0.092	0.781	0.072
4	0	-1	0.059	0.055	0.082	0.305	0.052